Bed Posture Classification using a Non-Intrusive Sensor System

For Prevention of Pressure Ulcers

Yanick Mampaey

Master of Science Thesis

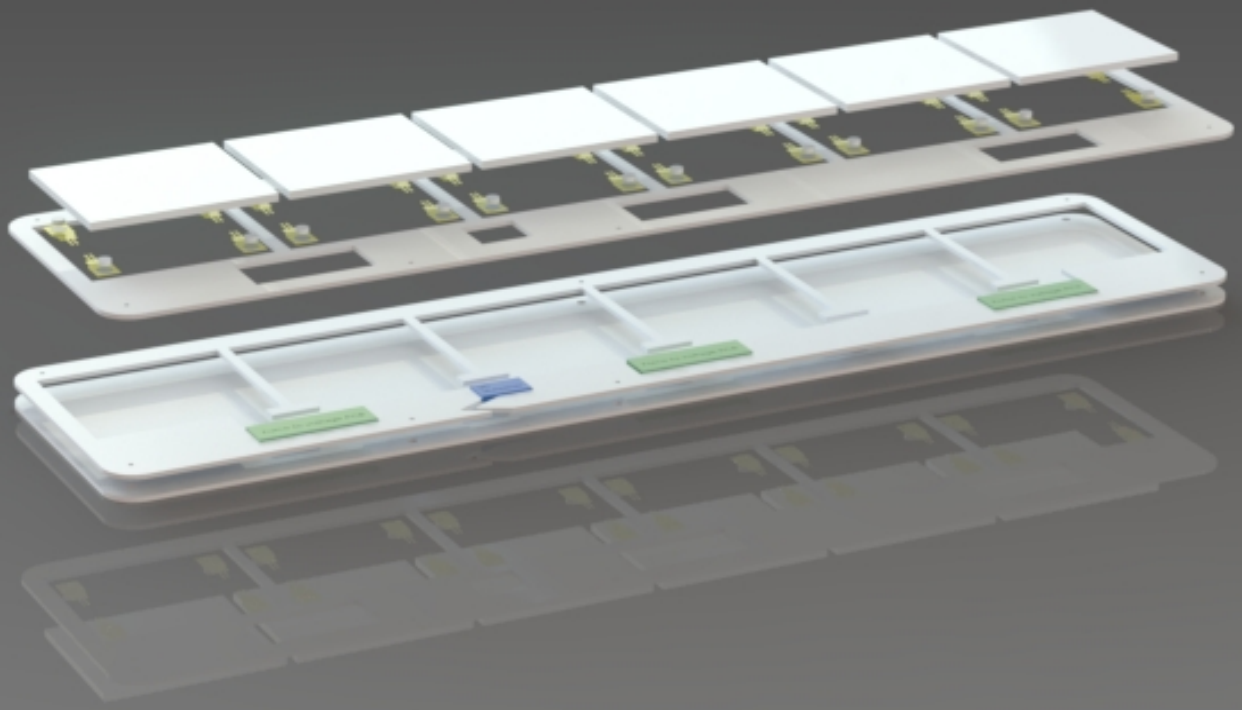

TU Delft Delft University of Technology

BioMechanical Engineering

Bed Posture Classification using a Non-Intrusive Sensor System

For Prevention of Pressure Ulcers

Master of Science Thesis

For the degree of Master of Science in Mechanical Engineering at Delft University of Technology

Author:
Yanick Mampaey

Supervised by:
Dr.ir. J. van den Dobbelsteen

January 6, 2019

Faculty of Mechanical, Maritime and Materials Engineering (3mE) · Delft University of Technology

The work in this thesis was supported by Momo Medical B.V. Their cooperation is hereby gratefully acknowledged.

Abstract

Background: Pressure ulcers are skin and soft tissue wounds that lead to severe patient suffering and considerable financial burden, with the yearly treatment cost estimated at 1.25 billion euro in the Netherlands alone. Research findings suggest posture classification in bed as a promising tool for pressure ulcer prevention, however currently no cost effective device is available that can accurately classify posture without being intrusive to the patient.

Objective: To develop a cost effective, non-intrusive sensor system and evaluate its effectiveness and classification accuracy.

Methods: A thin sensor system was developed which can be placed underneath a mattress at chest height of the patient. The sensor system has six rectangle plates, covering the width of the bedframe, that can measure the pressure gradient induced by the weight of the patient using 24 force sensing resistors, placed in the corners of the pressure capturing plates. Twenty-two test subjects were included in an experiment to create a posture measurements dataset. Data samples of eighteen subjects were used to train support vector machine classification algorithms for which the skewness, kurtosis and mean of the pressure distribution were used as features. Two algorithms were developed, the first to classify three postures and the second to classify five postures. The algorithms were then tested on the posture data of the four remaining subjects to determine the classification accuracies.

Results: Posture classification accuracy was 73.1% for distinguishing five postures and 84.3% for distinguishing three postures.

Conclusion: The findings suggest the feasibility of using a non-intrusive sensor system underneath a mattress for bed posture classification. Additional research is necessary covering the entire weight range of patients at risk of pressure ulcer development.

Preface and Acknowledgements

My time in Delft was a tremendous learning experience, with this thesis the final result. This had not been possible without the people that aided me during the process, for which I would like to express my gratitude.

First of all, I would like to thank my supervisor Dr. ir. John van den Dobbelsteen for his willingness to guide me during this project. Your pragmatic advice helped when the scope of the research was not yet clear. You were there when I needed you most and for that I would like to thank you.

Secondly, I would like to thank Menno and Ide for providing the opportunity to work at Momo Medical. It has been an incredible learning experience, both professionally as well as personally. Menno, your enthusiasm and drive are truly inspiring and Ide, your insight and critical thinking made your feedback always razor sharp. I wish you both the best of luck in the future.

Thirdly, I would like to thank the whole Momo Medical team for providing a fun and motivating work environment where new friendships were made and it definitely improved my table football skill. Furthermore I would like to thank my friends in Delft for all the fun we had during my studies and of course the 22 friends and colleagues who joined the experiments and laid on a bed for science.

Lastly I would like to thank my family and Liora, for their encouragement and incredible support along the way.

Table of contents

List of Figures

List of Tables

Chapter 1

Introduction

Pressure ulcers or pressure-induced skin and soft tissue injuries, develop when soft tissue over a bony region is continuously subjected to a mechanical load over time, resulting in tissue damage [30]. Pressure ulcers are among the most common encountered conditions for both acutely hospitalized patients and patients in need of long-term institutional care. It is estimated that there are 2.5 million pressure ulcers treated each year in acute care facilities in the United States alone [45] and that annually 60,000 patients die from pressure ulcer complications [14].

Pressure ulcers occur with a wide variety of patients, often causing severe pain, resulting in a prolonged hospital stay [19] and increasing the risk of premature mortality [8]. The costs of treating pressure ulcers in the Netherlands are estimated between 500 million and 2 billion euro annually, which is between 1,2% and 6,6% of the total health care costs [49]. The prevention of pressure ulcers is found to be cost effective over treatment and that it improves the quality-adjusted life-years of patients [6]. From both the patients and the hospitals perspective, all efforts reducing the prevalence of pressure ulcers is of great importance.

It is therefore interesting to investigate technological tools that could aid in the prevention of pressure ulcers. Chapter two of this thesis gives the background theory on the current technological state of the art in pressure ulcer prevention. It identified that monitoring a patients posture in bed reduces the prevalence of pressure ulcers, by notifying the caregiver when a patient is laying for a prolonged period of time in the same posture.

No sensor system is currently available that can detect patient posture while being cost effective and non-intrusive to the patient. First of all cost effectiveness can be obtained by limiting the amount of sensors. Literature indicated that an array of 16 sensors on top of a mattress is able to classify three postures, using properties of the pressure profile that correlate with posture [24]. However a sensor array on top of the mattress still has contact with the patient which could cause discomfort. Therefore it is proposed to place this sensor array underneath the mattess, with the hypothesis that similar pressure patterns can be detected. This states the main research question as:

How accurate can the lying posture of patients in bed be classified, using a cost effective, non-intrusive sensor system that is deployed underneath a mattress?

Chapter 2

Background

2.1 Etiology of Pressure Ulcers

The main mechanism causing a pressure-induced injury is the external pressure applied to the skin. However it is a combination of host-specific factors that determine the risk of pressure ulcer development. Factors contributing to the development of a pressure ulcer are: pressure, friction, shearing forces and moisture [48]. Furthermore malnutrition and weight loss are also contributing according to several studies [23, 33].

The severity of the pressure ulcer is classified by the National Pressure Ulcer Advisory Panel[1] in four stages, ranging from non-blanchable skin redness in stage 1 until a full range of tissue loss in stage 4, in which case bone becomes visible [2], as displayed in figure 2.1. There are two theories about pressure ulcers development that can be distinguished: top down or bottom up. The top down theory states a pressure ulcer starts on the surface of the skin and progresses deeper, whereas the bottom up theory states that a pressure ulcers starts in the deep tissue layers, since muscle tissue is the most susceptible to pressure induced damage compared to other soft tissues [38].

[1]The National Pressure Ulcer Advisory Panel (NPUAP) is and indipendant American organisation dedicated to the prevention of pressure ulcers. Together with the European Pressure Ulcer Advisory Panel (EPUAP) and the Pan Pacific Pressure Injury Alliance (PPPIA) they are publisher of the book "Prevention and Treatment of Pressure Ulcers: clinical practice guidelines" [2].

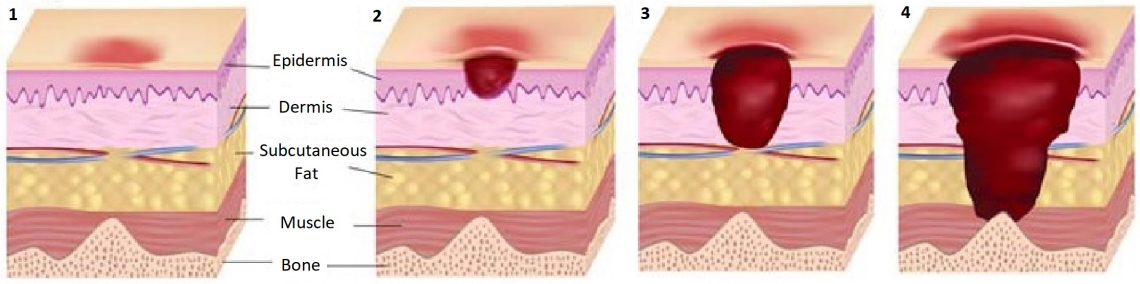

Figure 2.1: Pressure ulcer stages ranging from 1 to 4, source [31]

Pressure ulcers are most common on the sacrum (28%), heels of the feet (23.6%), ischial tuberosity (17.2%) [54] and are also seen over the heads of the long bones of the foot, at the hips, over the shoulder and over the back of the head [45].

2.1.1 Tissue Cells Reaction to Mechanical Loading

When an individual has contact with a surface, a mechanical load is induced in the underlying tissues, caused by the weight of the person and the reaction forces of the surface. This load can be divided into the normal force, perpendicular to the skin surface, and the shearing force, parallel to the skin surface. Both forces result in stress and strain within the affected tissues.

How this stress and strain affects the tissue is an inhomogeneous mechanism. It is dependent on the mechanical properties of the different soft tissue layers (skin, fat, muscle), their morphology and the external magnitude and distribution of the mechanical load. These properties also change during the lifetime of an individual due to ageing, lifestyle and health related issues. [2].

2.1.2 Tissue Cells Damage due to Mechanical Loading

Damage to the tissue depends on the time and magnitude of the external mechanical load that is applied. A low mechanical load applied for a long time as well as a high load for a short period of time will result in tissue damage. The time can be a matter of seconds, which is impact loading, or it can be a prolonged period of time, which is a sustained loading. It is sustained loading of the tissue that eventually causes a pressure ulcer. It is tested in early studies using animal models that a pressure of 70 mmHg applied on tissues for two hours can result in irreversible tissue damage [27] and later on Reswick and Rogers (1976) found an inverse relation between the allowable pressure and the duration of the applied pressure, indicating that higher load requires less time for tissue damage to occur [47]. However, the variety of individual parameters influencing the formation of pressure ulcers makes defining a damage threshold with surface pressure alone inaccurate [28]. Gefen et al. (2008) conducted an experiment with tissue engineered muscle and defined a relation between the damage thresholds of the muscle cells in relation with the compressive strain and the loading time [17], displayed in figure 2.2.

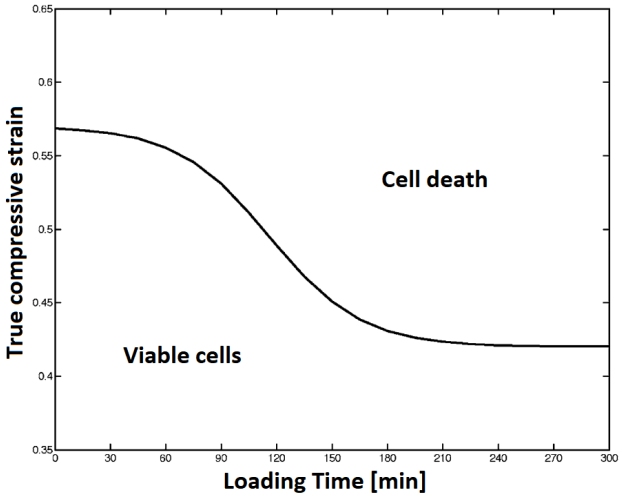

Figure 2.2: Soft tissue cell damage threshold of the compressive strain plotted against the loading time, adapted from Oomens et al.(2015) [40] and based on the findings of Gefen et al. (2008) [17].

Pressure ulcers are most common on the sacrum (28%), heels of the feet (23.6%), ischial tuberosity (17.2%) [54] and are also seen over the heads of the long bones of the foot, at the hips, over the shoulder and over the back of the head [45], as illustrated in figure 2.3. These are bony regions which cause pressure peaks in the surrounding tissue, shown in figure 2.4.

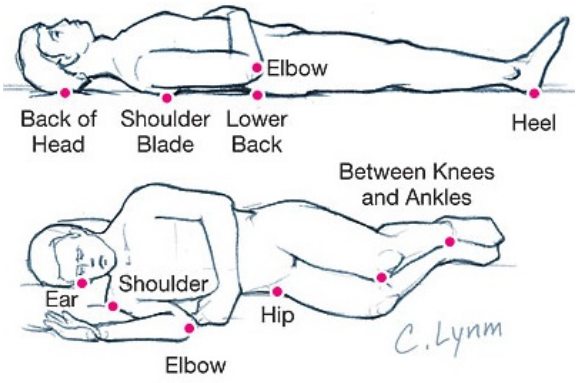

Figure 2.3: Most common locations of pressure ulcers, adapted from: Zeller et al. (2006) [58]

Research suggests that there are two important mechanisms that cause tissue damage due to mechanical loading. These are ischemia and direct deformation of the tissue cells.

Ischemia, the blockage of blood supply to tissue, obstructs the removal of waste products from the tissue cells and prevents them from getting nutrients and oxygen. Earlier research suggested that ischemia occurs beyond the internal pressure threshold of 32 mmHg, which is the arteriolar pressure [30]. There is a range however due to the time dependency of the pressure and the damage threshold varies between different soft tissues.

It is not yet clear how direct mechanical deformation of the tissue cells results in damage. Current theories suggest the stretching of the plasma membrane, stretching of the internal pathways or the direct rupture of the cytoskeleton causes cell death [2].

Other important parameters that influence the development of stage 1 and 2 pressure ulcers, are the temperature and humidity between the skin and the surface. This is also referred to as the microclimate. Here the skin becomes weaker and more elastic with increased humidity and temperature. The opposite occurs if the skin is too dry and the skin becomes brittle. Researchers are still debating over the optimal microclimate parameters [2].

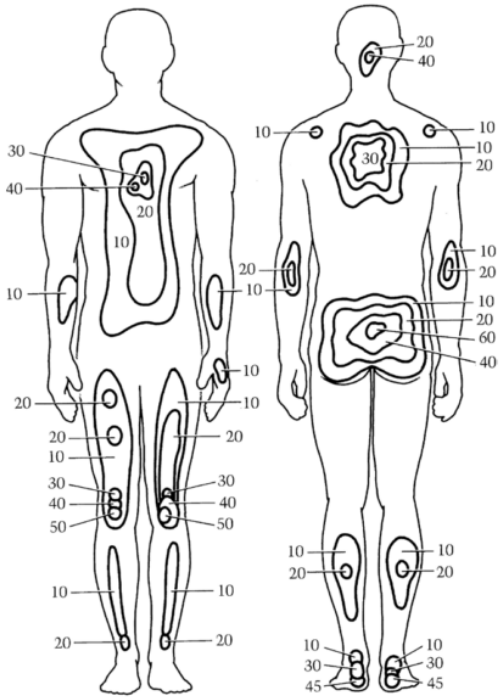

Figure 2.4: Interface pressure [mmHg] distribution in supine and prone posture, adapted from Tran et al. (2016) [54]

2.2 Risk Factors and Risk Assessment of Pressure Ulcers

The risk factors (see figure 2.5) can be divided into two classes: the intrinsic and the extrinsic factors. The extrinsic factors are the magnitude of the mechanical load, it's time duration and the types of loading. Intrinsic factors are individual parameters that need to be assessed when a patient is hospitalized and during hospitalization.

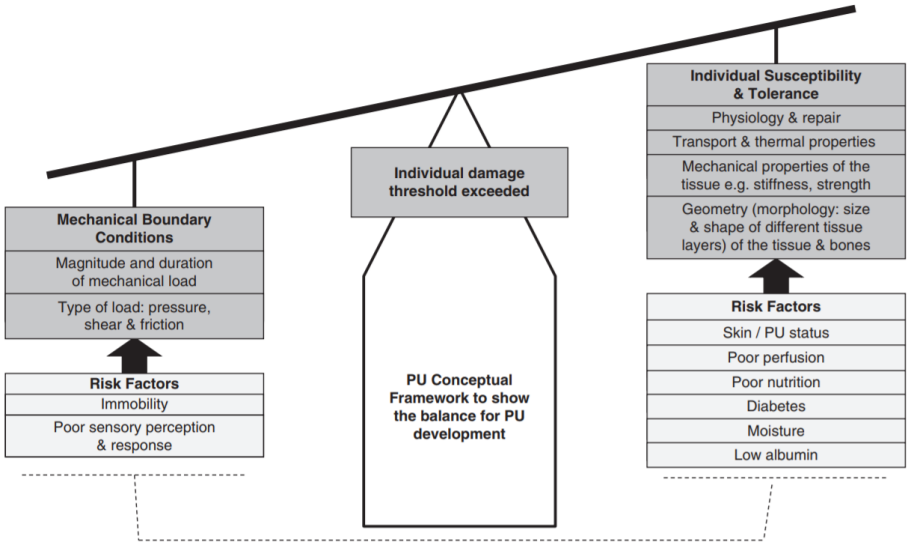

Figure 2.5: Pressure ulcer risk factors illustrated in a conceptual framework, adapted from Coleman (2014) [11].

Coleman et al. (2013) investigated the importance of each risk factor. They concluded that impaired mobility, impaired perfusion and pressure ulcers status were the three most critical risk factors. Other factors that indicate pressure ulcer risk are: age, nutrition, general health status, haematological measures and skin moisture [10].

To predict the probability of pressure ulcer development, a clinician uses its clinical judgement in combination with risk assessment tools. One downfall of the current risk assessment tools is that some risk factors are currently not included or graded, for example perfusion and oxygenation. Also the strength of the evidence is different for each risk factor. The most commonly used risk assessment tool is the Braden scale, developed in 1987. Moore et al. (2014) investigated the effectiveness of risk prevention tools. They found that there was insufficient evidence to prove that the risk assessment tools reduce the incidence of pressure ulcers over unstructured risk assessment [35].

2.3 Current Methods of Pressure Ulcer Prevention

When a high risk of pressure ulcer development with a patient is assessed, preventive methods are taken. The main prevention methods are repositioning patients, moisturising the skin on areas sensitive for pressure ulcer development, using support surfaces and optimizing the patient's nutrition.

Reddy et al. (2006) performed a systematic review containing 59 publications reviewing the current prevention methods. Their result was that with the current evidence the appropriate methods to prevent pressure ulcers are: repositioning the patient, usage of support surfaces, optimizing nutrition and moisturising the skin on the sacrum. However there is no information on the effectiveness of certain repositioning strategies over others and it is important to note that the methodological quality of the publications included where generally suboptimal and had important limitations. It is often not possible to blind the participants and it is also difficult to standardize certain aspects of the trial, for example hospitals have different "standard" mattresses and reposition protocols [45]. Patient repositioning and support surfaces will be discussed in further detail since those methods aim to directly alleviate the pressure on the patient.

2.3.1 Support Surfaces

The term support surface is intended for specialized mattresses, mattress overlays, and cushions. A support surfaces aims to distribute the weight of the patient and prevent localized pressure points on risk areas, which can be done actively or reactively. Reactive surfaces distribute the load as a reaction of the mechanical load and can be powered or non-powered. Examples are foam mattresses, air or gel filled mattresses/overlays, low air loss support surfaces and air-fluidized support surfaces. Active support surfaces actively change the weight supporting distribution of its surface and therefore needs to be externally powered. They use air filled cylinders perpendicular to the axis of the body as a basis for the support and they are inflated and deflated in an alternating pattern.

McInnes et al. (2015) investigated the effectiveness of using support surfaces that redistribute pressure. Reviewing 59 RCTs and quasi-randomised trial, they concluded that: "While there is good evidence that higher specification foam mattresses, sheepskins, and that some overlays in the operative setting are effective in preventing pressure ulcers, there is insufficient evidence to draw conclusions on the value of seat cushions, limb protectors and various constant low pressure devices. The positive effect of higher-tech constant low pressure and alternating pressure for prevention are unclear." [34]. McInnes also found the included trials to contain methodological flaws and to have a high risk of bias.

Oliveira et al. (2017) systematically reviewed the support surfaces used in surgical practice. They found a higher prevalence in patient's who did not have a specialized support surface compared to standard foam mattresses [12].

2.3.2 Patient Repositioning

In clinical practice protocol it is common to reposition patients at risk of developing pressure ulcers within a time interval ranging from two to four hours. The patient is repositioned from one to another of the following postures: a supine posture (0°) and two lateral postures on both sides (lateral 30° supported with cushions or lateral 90°). To prevent pressure peaks which can occur

with the lateral 90° posture, the lateral 30° is preferred according to the NPUAP clinical practice guidelines [2].

Gillespie et al. (2014) stated that best practice guidelines recommend the two hour interval and they identified that: "These recommendations appear to be based on small studies (not RCTs) conducted 20 or more years ago, that either compared different repositioning schedules or repositioning schedules with no manual repositioning (spontaneous body movements) (Exton-Smith 1961; Norton 1962; Palmen 1987; Smith 1990). The usefulness of these studies for today's decision making is further compromised since the standard of hospital mattresses has greatly improved since then" [18].

Figure 2.6: Lateral 30° posture, adapted from NPUAP-EPUAP-PPPIA (2014) [2]

Studies however not yet succeeded to identify an optimal repositioning strategy. Bergstom et al. (2013) conducted a randomised clinical trial investigating the difference between a two, three and four hours interval of repositioning with 942 participants for three weeks and no difference was observed in pressure ulcer incidences, between the different invervals [7]. Zeh et al. (2015) performed a systematic review on optimal repositioning tactics and could not identify a single RCT or controlled clinical trial that had meaningful evidence on the effectiveness of repositioning [57]. Despite the lack of hard evidence, expert opinion is in favour of repositioning and it was unambiguously agreed upon on the NPUAP conference in 2011 that support surfaces will not be able to replace repositioning [9].

2.4 Technologies for Pressure Ulcer Risk Monitoring

A variety of sensor systems are proposed which are hypothesized to monitor individual pressure ulcer risk factors. Marchione et al. (2015) summarized the different methods of software approaches monitoring risk factors for pressure ulcers. They found 36 publications which used a variety of monitoring methods. The different risk factors that are investigated are pressure, temperature, humidity and blood flow. A variety of sensor techniques are used to provide reports on the interface pressure, interface temperature, interface humidity and the body posture. Feedback to the caregiver is mostly performed by alerts in the form of light, sound and text messages. Two approaches perform pressure management by mechanically actuating compartments of a segmented bed when a prolonged pressure is measured, to redistribute the pressure [32].

There are limitations with the sensor systems identified. Most sensor systems proposed are prototypes and have a low technology readiness level. This also implies that there is little or no evidence provided to proof that the sensor systems are effective in pressure ulcer prevention. Another limitation is that most systems require patient contact, and little information is given about patient comfort and hygiene. This limits clinical applicability of some technologies.

In more recent literature there are three clinical trials identified which provide evidence for their effectiveness in pressure ulcer prevention. They are based on monitoring interface pressure and the posture in time respectively. These technologies, namely continuous bedsite pressure mapping and monitoring the patients body posture through a wearable sensor, will be further explored in the next sections.

2.4.1 Continuous Bedsite Pressure Mapping

Continuous bedsite pressure mapping uses a pressure sensing mat or mattress to measure the patients interface pressure and visualizes this in a heatmap. This information is then provided to the caregiver and it is hypothesized that this will improve the repositioning practice by reducing interface pressure due to visual pressure feedback to the caregivers.

In terms of compliance to the repositioning protocol, Motamedi et al (2013) found in a small study of 9 patients that when using a continuous bedsite mapping device the repositioning frequency was 0.491 (SD, 0.271) compared to a repositioning frequency of 0.325 (SD, 0.235) without the sensor system [36].

Walia et al. (2016) identified two cohort studies which had as primary outcome the amount of hospital acquired pressure ulcers and pooled the data to perform a meta-analysis. One had a prospective study design [5]and the other a retrospective [50], which combined had a patient population of 1049, with 520 patients who had a pressure monitoring device installed next to their hospital bed and a control group of 529 patients who received standard care. Since the patient group was homogeneous, a fixed-effects model was used for meta-analysis, this resulted in a significant pressure ulcer risk reduction of 88% (Mantel-Haenszel RR 0.124; 95% CI, 0.038-0.407).

Gunningberg et al. (2017) performed a RCT which also investigated the usage of a pressure mapping system with as primary outcome pressure ulcer incidence. The study was performed in a geriatric ward and included 190 patients, of which 150 had no pressure ulcers upon admission. In the intervention group there were seven out of 69 (10.1%) that developed pressure ulcers during their stay, compared with seven out of 81 patients in the control group. (8.6%), resulting in an incidence ration of 1.13 (95% CI: 0.34–3.79) [20]. Gunningberg proposed that a possible reason for this outcome could be the increased awareness of the staff, affecting the pressure ulcer prevalence

in both groups.

Continuous bedsite pressure mapping has significant evidence from cohort studies with a larger sample size, however it is not confirmed by a RCT. It could be possible that the incidence reduction in the studies included in the meta-analysis of Walia et al. is caused by an increased compliance to protocol rather than to interface pressure reduction. Further research in terms of a larger sized RCT is needed to confirm this finding.

2.4.2 Wearable Posture Sensor

Body posture monitoring can track the time that tissue is subjected to pressure on a certain side of the body, assuming standard postures of patients in bed correlates with pressure peaks in anatomical locations at risk. Technologies that are developed are a chest belt which uses an accelerometer [46] or a wearable sensor developed by Leaf Healthcare, which sticks to the chest of the patient [43].

Pickham et al. (2017) performed a RCT with a sample size of 1312 patients that underwent allocation in two intensive care units, to assess the clinical effectiveness of the wearable sensor developed by Leaf Healthcare. The primary outcome was the amount of hospital acquired pressure ulcers and the secondary outcome was the compliance to the repositioning protocol. Every patient got a wearable sensor that tracked the patients position through time and the intervention group had information feedback to the caregiver. The information they received was the quality of the repositioning performed, patient's current posture and the time until the next turn. The wearable sensors in the control group only recorded posture data and did not send any information feedback. Blinding was adequately performed if possible, a Fisher's Exact test was used to analyse intention-to-treat and per-protocol effects were analysed. Incidence rate was 0.76% in the intervention group and 2.3% in the traditional care control group. This results in a significant prevention of pressure ulcers using the feedback from the wearable posture sensor (OR=0.33, 95% CI [0.12, 0.90], p=0.031) and the compliance rate to turning protocol was significantly different as well between the intervention and control group (67% vs 54%; difference 0.11, 95%CI [0.08, 0.13], $p < 0.001$). Furthermore there was no significant difference between the turning angles and depressurization time between patients groups [43].

Pickham et al. (2017) provided the first evidence based indication, that the use of bed posture feedback to the nurse increases the compliance rate to the repositioning protocol, which correlated to less pressure ulcer incidences. It is to be noted that the compliance rate to protocol of 67% leaves room for further improvement, even with visual reminders as feedback to nurses. More research is needed in how the repositioning practice can be optimised in terms of repositioning frequency, how the compliance rate can be further increased by other type of reminders (using sound/text message) and wat the limitations of the compliance might be in terms of available staff. Being one of the largest sized trials, followed with a strict study protocol, this is currently the best evidence available on how technology can improve the repositioning practice.

Table 2.1: Evidence found in literature of the technological developments quantifying effectiveness regarding pressure ulcer prevention.

Technology	Id	Author	Study design	Method	n	Results
Continuous bedsite pressure monitoring	[55]	Walia et al. (2016)	Meta-analysis	A meta-analysis of two cohort studies that used continuous bedside pressure mapping to assist during repositioning.	1049	There was a significant reduction of 88% in risk of developing pressure ulcers (Mantel-Haenszel risk ratio, 0.12; 95% confidence interval, 0.04–0.41; I^2 =0%).
	[20]	Gunningberg et al. (2017)	Randomised controlled trial	A bedside pressure mapping system displaying patients pressure points is used in the intervention group to give visual feedback to the caregiver during repositioning. Both intervention and control groups received standard care.	190	No significant difference in the prevalence of pressure ulcers was seen between the intervention and the controll group, with an incidence rate ratio between the intervention and control group of 1.13 (95%CI: 0.34-3.79).
Wearable posture sensor	[43]	Pickham et al. (2017)	Randomised controlled trial	Optimal repositioning practice determined from real-time data from a wearable posture sensor is compared with traditional repositioning practice.	1312	Incidence rate was 0.76% in the intervention group and 2.3% in the traditional care control group. This results in a significant prevention of pressure ulcers using the feedback from the wearable posture sensor (OR=0.33, 95% CI [0.12, 0.90], p=0.031).

2.5 Non-Intrusive Bed Posture Detection

In section 2.4.2 it is shown that measuring the posture of a patient in bed using an accelerometer on the chest and providing this feedback to the caregiver, decreases pressure ulcer prevalence. However this measuring method induced patient discomfort, since direct contact between the patient and the sensor was needed. In this section the state of the art of body movement detection in bed will be reviewed to investigate non-intrusive alternatives for posture detection.

The movement of the human body in a bed has been studied in a variety of research fields. Signals from the body vary from small movement, like arterial pulses caused by heartbeat, to large movement caused by the body limbs. The different levels can be viewed in figure 2.7. Posture is the most relevant parameter for this research and there are two main parameters that can be distinguished: the exact posture at a given time and the time a posture change occurs. Measuring exact posture is preferred for pressure ulcer prevention shown by Pickham et al. (2017) [43]. Initial research identified the following main sensory methods of non-intrusive posture detection:

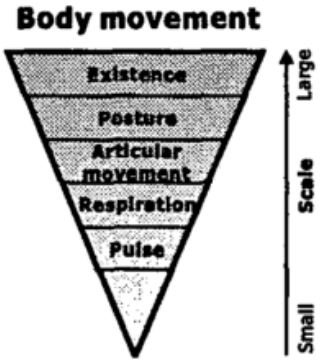

Figure 2.7: Body movements from small to large, adapted from Harada and Mori (2002) [21]

- Camera
- Radar
- Load cells
- Piezoceramic sensors
- Force sensing resistors

The publications often measure signals caused by the human presence in a bed, using a sensor technology and evaluated the correlation to a reference signal. This however is in practice a hard underdetermined problem to solve. Due to sensor limitations and the high amount of variables in the system, including patient, bedframe and mattress variations. Furthermore it is difficult to measure a single parameter of body movement, since every other body movement induces noise in the signal measured.

Due to the system complexity, noise and limited information, most publications for posture detection use a combination of signal filtering and classification techniques. A measured sensor signal is analysed and properties (features) are extracted that are hypothesized to correspond with body posture or movement. These features of a sensor data set are used to train a classification algorithm, in combination with a reference data set (labels). The accuracy of the algorithm is then determined by making a classification prediction on a validation data set.

2.5.1 Sensor Technology Choice

The technologies are systematically graded stating advantages and disadvantages, after which a choice will be made. The exclusion criteria will be factors that prohibit implementation in a hospital environment. The grading criteria are the achieved accuracy on determining exact posture, the cost effectiveness and ease of implementation as a standalone device.

Camera Camera systems can detect posture change and respiration rate [37], however due to patient privacy regulations it is not feasible to deploy a camera setup next to a hospital bed.

Radar Radar technology works with two radars placed underneath a mattress that detect vibrations in the human body according to the Doppler effect. It is mainly accurate at measuring heart rate [26], but there is not much literature in exact posture detection. Since it requires two quality radars, with estimated costs around 500 euro each, it is not a cost effective method.

Loadcells Using four loadcells under each bed support, the total load as well as small vibrations can be measured. Using the sum of the four loadcells, Adami et al. (2005) trained a classifier to distinguish small from large movement with an accuracy of 95% [3]. Beattie et al. (2011) used the information of each loadcell to determine the center of pressure in the x and y axis of the bed [4]. They were able to filter out the breathing rate and hypothesized that the breathing angle in the xy plane, which they calculated from the center of pressure, was different for back, left, right and stomach posture. With an average accuracy of 84% for differentiating 3 postures this is reasonably successful.

The downside however is that the patient must remain still, since large movement induces noise to the extent that respiration cannot be detected. The second downside is that the sensors are placed underneath the bed supports. Making installation as a standalone device difficult.

Piezoceramic sensors Nukaya et al. (2012) investigated the use of piezoceramic sensors that, comparable to the loadcells, were placed underneath the bed supports [39]. These sensors are sensitive to mechanical vibrations. No classification was performed, however the signal was analysed and visually compared. This gave indication in the possibilities to detect respiration rate, heartbeat, changes from lying to sitting and articular movement like scratching.

Force sensing resistors A force sensing resistors (FSR) electrical resistance changes when a load is applied. They are mostly setup in a matrix formation, allowing to measure pressure over an area with a resolution specified by the amount of sensors in the matrix.

Two publications investigated the use of pressure sensing for movement detection underneath a mattress. Foulbert et al. (2012) detected with 100% accuracy transitions between lying and sitting using a sensor mat covering the whole area underneath the mattress [16]. Townsend et al. (2009) detected 83% of patient roll-overs. The algorithm was based on the center of gravity, calculated from a matrix of 8x3 FSR's at different locations underneath the mattress.

For exact posture determining, seven publications were identified, shown in table 2.2, all which measured on top of the mattress. One measured using a one dimensional array of 16 FSR's [24] and six publications measured using a two dimensional pressure sensing matrix [25, 56, 29, 44, 42, 22]. A variety of algorithms were developed going from basic machine learning methods such as linear

support vector machines and k-Nearest Neighbours to deep neural networks with vary accurate results, seen in table 2.2.

The disadvantages of force sensing resistors for the exact posture determination, is the sensors were placed on the top of the mattress, staying in contact with the patient. Furthermore a single force sensing resistor is not expensive, however a commercially available sensor mat of the size and resolution uses in the found publications can cost up to 10,000 euro.

Table 2.2: Accuracy in posture detection for literature measuring exact postures.

Id	Author	Resolution	Algorithm	Postures	Accuracy
[24]	Hsia et al. (2008)	16	Bayesian classifier	3	78.70%
[25]	Hsia et al. (2009)	56	PCA, SVM	5	95.00%
[56]	Yousefi et al. (2011)	2048	PCA, ICA	5	97.70%
[29]	Liu et al. (2013)	8192	Sparse Classifier	6	83%
[44]	Pouyan et al. (2013)	2048	kNN	8	97%
[42]	Ostadabbas et al. (2014)	1728	kNN	3	98.40%
[22]	Heydarzadeh et al. (2016)	2048	HoG + DNN	5	98.10%

A grading table, see table 2.3, was used to evaluate the technologies on the aspects of patient privacy, posture detection capability, cost and clinical implementability. Camera systems perform generally well, yet they are excluded for privacy regulations. Radar technology performs well on measuring small scale body movement, yet has little evidence on posture detection and is not deemed cost effective. This leaves loadcells, piezoceramic sensors and force sensing resistors for further evaluation.

Loadcells and piezoceramic sensors have comparable measuring an sensor characteristics. They are low cost, yet due to the difficulty of incorporating the sensors underneath a hospital bed and inaccuracy with small patient movements they are not an ideal solution and therefore score low on implementability.

Very accurate results have been achieved with FSR's setup in a high resolution sensor mats on top of the mattress. However the cost of such a mat is not feasible for each bed in a hospital. It also induces some discomfort as these mats need to be in contact with the patient and are filled with electronic components.

Table 2.3: Grading table for de possible sensor types, graded from 1 (low) to 3 (high).

	Camera	Radar	Loadcells	Piezoceramic	FSR
Patient privacy	1	2	3	3	3
Posture detection	3	1	2	1	3
Cost	2	1	3	3	2
Implementable	2	2	1	1	3
Total	8	6	9	8	**11**

The cost of the sensor mat is highly correlated with the amount of sensors in the mat. It has already been shown that using a limited amount of sensors set up in an array, an accuracy could be reached of around 80%. This algorithm was based on skewness and kurtosis of the force curve measured. Furthermore it is shown that when measuring pressure underneath the mattress,

movement change can be detected. Using a limited amount of sensors and placed underneath the mattress, FSR's match the criteria cost effectiveness and non-intrusiveness for the patient. The main goal of the thesis will be to develop such a sensor system and to determine the classification accuracy for posture detection.

2.6 Background Conclusions

Pressure ulcer risk can be described as a balance between the individuals susceptibility and the mechanical load applied. If the mechanical load outweighs the individual tolerance, tissue damage will occur. The mechanical load, consisting of normal, shear and friction forces cause a compression of the internal tissue layers. The individual tolerance is determined by the morphology of the fat, muscle and skin tissues, their difference in mechanical properties and the cell physiology of the individual. The most important patient risk factors are identified as impaired mobility, impaired perfusion and earlier pressure ulcer status.

Due to the variation of the load over time and the amount of parameters influencing the patients tolerance, it is highly case specific as to when tissue damage occurs and it is impossible to precisely predict using a generalized model.

The current prevention methods are focussed on minimizing the mechanical load on the soft tissues. This is done by using specialized support surfaces or by repositioning the patient. Specialized support surfaces provide an even pressure distribution, minimizing pressure peaks and some specialized support surfaces also provide automatic redistribution of pressure using automated air pump systems.

However, when a patient keeps lying in a single posture there is no complete pressure relief. Repositioning is the act of changing the patients posture, relieving the previous posture from pressure and allowing it to recover. There is a lack of evidence on the effectiveness of repositioning, nevertheless it is expert opinion that support surfaces cannot replace repositioning.

There are two technologies proposed for monitoring pressure ulcer risk: continuous bedsite pressure mapping and a wearable posture sensor. The results are unclear for the effectiveness of continuous bedsite pressure mapping. A wearable posture sensor did provide evidence for minimizing pressure ulcer prevalence and improving compliance to the repositioning protocol. The sensor however was still intrusive and is not ideal for every patient type, due to the fact that it was attached to the chest of the patient.

Other alternatives for non-intrusive posture detection were researched. From five measuring technologies, force sensing resistors were chosen as a starting point for the sensor design. They show promising feasibility for posture detection, are cost effective and can be placed underneath the mattress, which is non-intrusive for the patient. The research question of the thesis will be: "How accurate can a patients bed posture be classified, using a low cost sensor system underneath a mattress?"

Chapter 3

Methods

The background research identified patient posture feedback to the caregiver as a method for pressure ulcer prevention, with the main requirements beïng cost effectiveness and non-intrusiveness for the patient. From the technologies investigated, force sensing resistors (FSR's) were the most promising technology (see section 2.5.1 and table 2.3), which met the requirements when a limited amount of sensors are placed underneath the mattress.

Previous bed posture classification literature achieved promising results by using FSR's above the mattress and the hypothesis for this thesis is that a comparable signal above the mattress can be measured underneath the mattress. The purpose of this thesis is to develop a sensor system to measure these signals and determine its posture classification accuracy.

3.1 Clinical Requirements Analysis

For sensor development in a medical setting it is important to consider design requirements from the clinical perspective. The first is that a considerable amount patients should be monitored to effectively reduce pressure ulcers on a large scale. The fastest way to implement posture monitoring, is to develop a cost effective sensor system that requires the least amount of adaptation in the current hospital infrastructure and working methods of the caregivers. This would require a standalone device, which is easy to install, applicable with standard bed frames and mattresses.

Furthermore, the sensor system should not be intrusive for optimal patient comfort. Non intrusiveness means that the patient should not be able to feel the presence of the sensor system underneath the bed. Components underneath the mattress require space and it's presence will be felt if there is a localized elevation caused by the sensor system size. This requires a limited sensor system thickness. It is estimated that a a rigid piece of material with a thickness of 15mm can be felt underneath the mattress so this is used as an upper bound.

A large patient weight range from 30kg to 170kg is proposed since both severely underweight and overweight patients are considered to be at risk of pressure ulcer development.

The postures relevant for repositioning are based on the clinical practice guidelines found in section 2.3.2. These include 5 postures: lateral 90° left, lateral 30° left, supine 0° , lateral 30° right and lateral 90° right. The statements above can be summarised in the following requirement list:

- Non-intrusive for the patient, limiting thickness to maximum 15mm
- A patient weight range of 30kg to 170kg
- Detect the five postures relevant for repositioning
- Compatible with different support surfaces and a variety of hospital beds
- Cost effective
  - Small amount of sensors, limiting hardware costs
  - Work as a standalone device, reducing implementation costs

3.2 Feature Hypothesis for Bed Posture Classification

For bed posture classification, it is necessary to hypothesize signal characteristics or features in the pressure signal that could correlate to different postures. Features will be easier to distinguish from a higher quality signal, which increases with the amount of force sensing resistors (FSR's), higher quality FSR's and more area being measured. This however results in higher cost so a compromise had to be made between the low cost requirement and the accuracy of posture detection.

In general, all the load of a patient in a bed is distributed over the surface of a mattress, with the mattress supported only by the bedframe. This means that the total pressure on top of the mattress must be equal and opposite to the pressure on the bedframe. The mattress has characteristics of a spring-mass-damper system but due to the 3D compression properties of foam and variation in foam layers, the pressure distribution on the bedframe is a nonlinear transformation of the pressure distribution on top of the mattress. It is the hypothesis that although the pressure distribution is transformed, similar features can still be detected to classify posture. To estimate this pressure distribution it is necessary to first determine the amount of FSR's and their location.

Due to a cost constraint only a limited amount of sensors will be considered. With a small amount of sensors available, it is necessary to investigate the most efficient locations of those sensors, which would be were most of the pressure and pressure gradients can be detected. Figure 3.1 shows the interface pressure on top of the mattress for five different postures. The first observation is that the highest pressures are measured around the shoulders and the hips. The second observation is that the center of pressure of the patient in x direction is varying for different postures while this is less the case for the y direction. Features can be based on those variations, which means that measuring with an array of force sensing resistors in x direction is the most efficient.

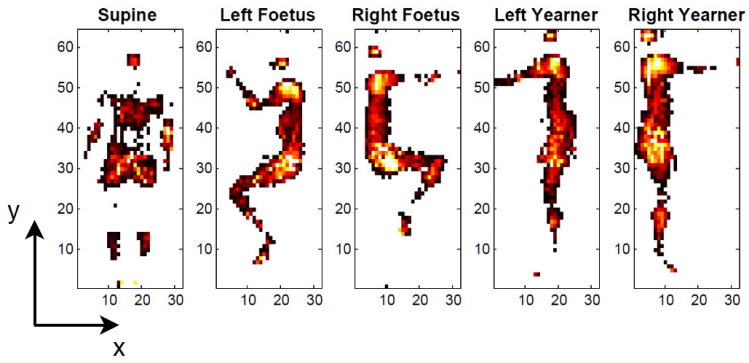

Figure 3.1: Five postures viewed from pressure images, which are used in the classification of Yousefi et al. (2011) [56].

Another reason to measure in an array along the x axis is that most hospital mattresses have a rigid bedframe with three hinges, over which a rigid sensor system cannot be placed. From an implementation standpoint this leaves three feasible sensor system locations: underneath the legs, underneath the sacrum and underneath the upper chest. Since the most information can be seen underneath the shoulders and the hips, the legs will not be considered as a sensor system location.

The location underneath the shoulders is chosen over the hips due to the assumption that for different patient lengths the location of the shoulders has less variation in y direction compared to

the location of the hips. The shoulders are close to the cushion, which usually lies on the same location and therefore serves as a reference point. Furthermore this location is assumed to contain the most posture information since the torso is the widest part of the body and pressure induced by the arms can be detected as well. The sensor location on the hospital bed used in the experiments of this thesis is shown in figure 3.2.

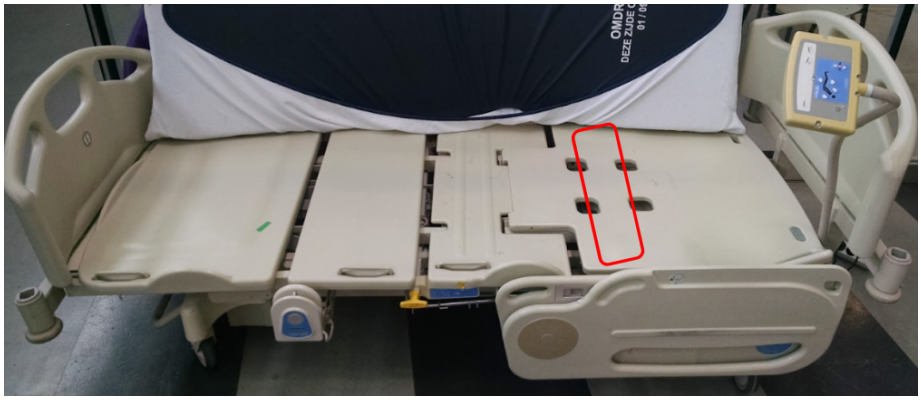

Figure 3.2: Standardized hospital bed produced by Hill-Rom which is used in the experiments, with the sensor system location indicated by the red rectangle.

Hysia et. al. (2008) researched posture classification at this location on top of the mattress, using an array of 16 FSR's [24]. They calculated the skewness and kurtosis of the pressure distributions per posture and used them as features for the classification. The hypothesis was that a supine posture evenly distributes the pressure along the width of the mattress, resulting in a low kurtosis and no skewness. The left and right postures were assumed to have a higher kurtosis due to a pressure peak from the shoulders and respectively be negative or positive skewed due to additional weight of the arms. Pressure measurements indicated a visual representation of these effects and a decent classification result of 78% was achieved.

Assuming the same characteristics can be seen underneath the mattress, a minimum sensor amount to detect these features can be reasoned as five, in case the sensors are sufficiently accurate. If evenly spaced across the width, five sensors would give an indication about the center force, the outer forces and the ones in between. In an ideal situation with a patient lying in a supine posture in the middle of the bed, it is hypothesized that sensor one and five have a low reading, sensor two and four have a similar reading caused by lying under the shoulders and the arms and sensor three would have a slightly higher reading caused by the weight of the chest, illustrated in figure 3.3. A lateral right side posture for a centered patient in bed would then cause a dip in sensor one and two and a raise in sensor three and four, where a lateral left side posture is assumed to have a mirrored pressure distribution.

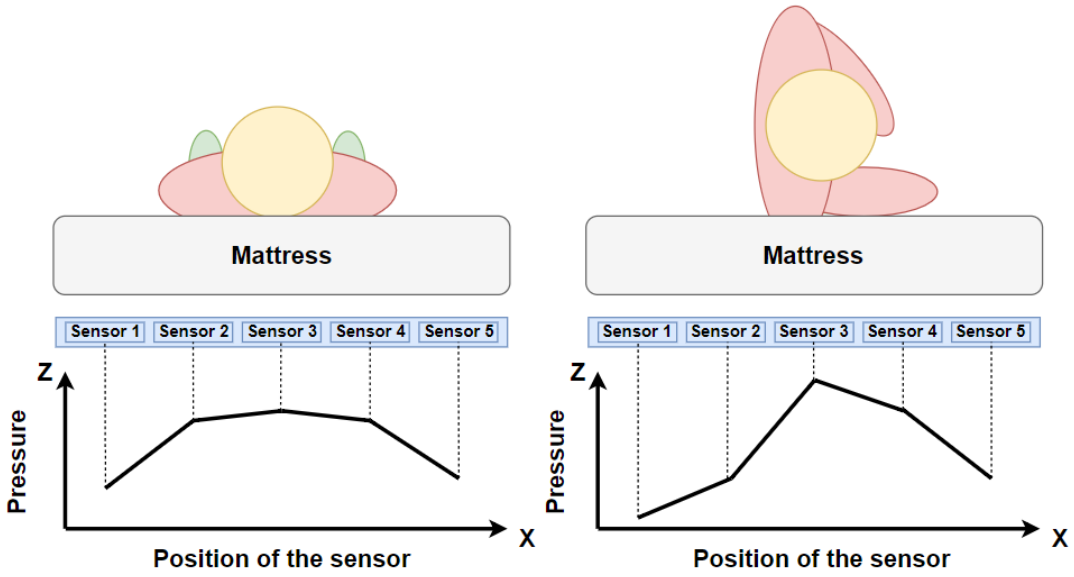

Figure 3.3: Hypothesized pressure signal characteristics for a supine (left) and lateral right posture (right).

However, more data points then five are preferred, since this allows more subtle pressure distribution changes. FSR's are unfortunately prone to sensor errors like hysteresis and non-linearity effects. Another factor that determines this pressure distribution is the amount of area measured per sensor.

For the sensor system development, it was therefore chosen to further analyse these design parameters and perform initial testing as a preliminary validation that the pressure distribution patterns can be seen underneath the mattress.

(3.1)

3.3 Sensor System Development

3.3.1 Force Sensing Resistor Choice and Initial Testing

In this section there will be explained which force sensing resistors (FSR's) are chosen for implementation in the sensor system design. First the FSR type will be chosen and then a readout circuit is designed to do initial testing. This initial testing has the purpose to identify the sensor characteristics of variation in mechanical load, as well as to measure the pressure underneath the mattress as a reference measurement for further development.

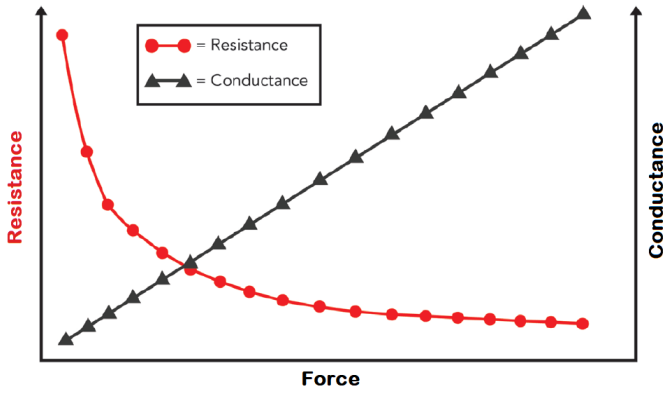

Figure 3.4: Graph showning the effect of increasing force on a FSR, resulting in a resistance decrease and a linear increase of the conductance, source [53].

A FSR is in essence a resistive polymer between two electrodes. The resistive property is caused by granules in the polymer structure. When force is applied, these granules are compressed and contact area between them increases, allowing for more efficient routes for the flow of electrical current and therefore a resistance decrease, corresponding with a linear conductance increase.

There are two main manufacturers of affordable and thin force sensing resistors. These are the FSR made by Interlink Electronics and the Flexiforce made by the company Tekscan. While the Interlink FSR sensors are robust, it is general consensus that they lack accuracy and precision as well as having quite some temperature drift compared to the Flexiforce sensors.

Since sensor accuracy and precision are important factors for measuring the pressure profile, the Flexiforce sensor is chosen to be incorporated into the sensor system. The Flexiforce sensor can be ordered in 4 force ranges: 4.5N, 110N, 445N and 4448N.

To measure pressure underneath the mattress a small and thin scale is proposed, build up from thin plate material and four Flexiforce sensors. The area of this scale is known and therefore the pressure can be determined. This sensor can be placed at different locations underneath the mattress to investigate localized pressures. For this scale a small surface area is chosen, since this will give the best indication about localized pressures. Therefore the lowest 4.5N range is chosen for initial testing, as these are assumed to have the best fit with the load range underneath the mattress, for a small surface area and would be the most sensitive to load variations. The sensor systems FSR's force range were later determined according to these initial test results.

Figure 3.5: Flexiforce A301 sensor, source [51].

Sensor readout circuit

To receive a reading from the sensor a readout circuit was designed. This circuit needs to be setup in such a way that a relation between the force pressing on the sensor and a measurable output parameter is achieved. Voltage is generally chosen as a reference parameter since this is easily detectable and converted to a digital signal. It is known that force sensing resistors can, as the name suggests, be placed in a circuit as a variable resistance. A voltage reading can be achieved by using the FSR as the variable resistance of an inverting opamp circuit. This analogue voltage output can be then converted to a digital reading using an analogue to digital converter (ADC). The digital signal is then sent to a computer via a raspberry pi and ethernet connection.

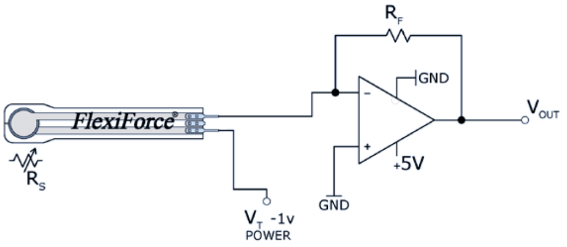

Figure 3.6: Force-to-voltage circuit to readout the Flexiforce sensor, source [52].

The inverting opamp ciruit is shown in figure 3.6. Applying force on the sensor results in a change in sensor resistance. The resistance at zero force is around $20M\Omega$ and when force is applied this resistance is lowered. With an inverting opamp circuit, the following relation exists between the output voltage and the sensor resistance:

$$V_{out} = -V_T * \frac{R_f}{R_s} \tag{3.2}$$

With V_T the supply voltage, R_s the Flexiforce sensor variable resistance and R_f a fixed resistor value. The maximal rated current for the sensor is 2.5mA and therefore the maximal supply voltage for the 1lb Flexiforce sensor is recommended at -1 volt.

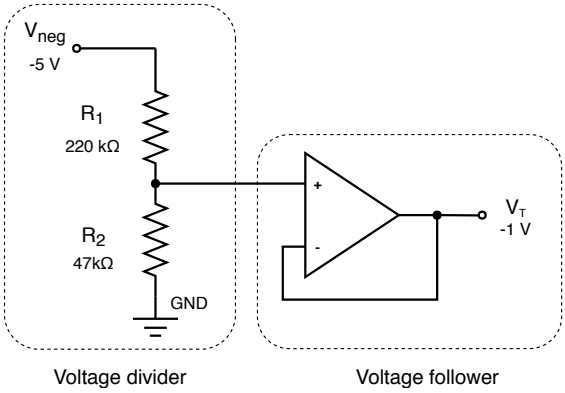

Figure 3.7: Voltage divider and voltage follower circuit.

The supply voltage of the Raspberry Pi is +5 volt (V_{CC}), so a negative -1 voltage can be created by a using a voltage converter, voltage divider circuit and a voltage follower circuit, see figure 3.7. The positive voltage of +5 volts can be converted to a negative -5 volts with a voltage converter. A voltage divider was setup to lower V_{neg}. The voltage divider has the following relation for the output voltage:

$$V_T = V_{neg} * \frac{R_2||R_{load}}{R_1 + R_2||R_{load}} \approx V_{neg} * \frac{R_2}{R_1 + R_2} \tag{3.3}$$

Because V_T is used as a stable power supply a voltage follower is also needed. Without a voltage follower, the system load which can be expressed as a resistance, would be parallel to R_2. An opamp

set up a voltage follower, as seen in figure 3.7, has a very high impedance, which acts as a very high resistance in a DC circuit. Therefore R_{load} in equation 3.3 can be ignored and resistor values R_1 and R_2 can be chosen as 220 kΩ and 47 kΩ respectively, so that a factor of around 1/5 is achieved. Resulting in $V_T = 0.18 * V_{neg}$.

The next step is to determine the fixed resistor value. R_f mainly determines the gain factor, and it should be chosen together with the ADC gain in such a way that the highest range can be detected by the ADC. The load range is determined by the expected signal to be measured and the ADC resolution is determined by the audio bit depth. For the experimental setup this was achieved by applying the highest load range, setting the gain of the ADC to the highest voltage range of (gain of 2/3) and then iteratively determining the resistor value which gave the highest amplification without falling out the voltage range. This resulted in an R_f of 22 kΩ.

This is later on expanded to a larger setup which can readout up to four sensors. Using one voltage converter, one ADC and four inverting opamp circuits for each sensor, shown in figure 3.8.

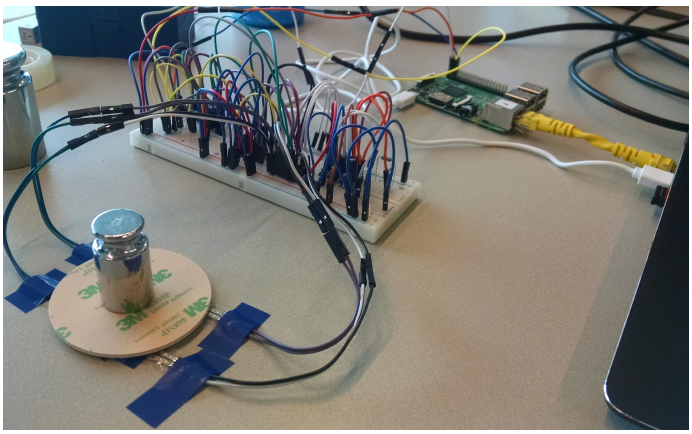

Figure 3.8: Breadboard configuration which can readout four sensors.

Applying Load and Testing Precision

Once a readout system was setup, load variations can be applied on the sensor for initial testing. The entire sensing area of the Flexiforce sensor is treated as a single contact point. The manufacturer of the FSR's recommends an even distribution of the load above the sensing area. Readings may vary if this load distribution changes.

Furthermore it is recommended to place the footprint of the applied load centred on the sensing area and that the entire load path of the applied load goes through the sensor. The loads applied during initial testing are dead weights with a bottom surface area larger than sensing area, so in order to measure the entire load a puck can be used.

A puck is a small piece of rigid material, which is placed centered in the sensing area of the sensor. By making sure the load is only supported by the puck and the puck is only supported by the sensing area, it is prevented that a part of the load is supported outside the sensing area. This allows the whole load to be measured.

Precision or reproducibility of a reading is an important sensor characteristic in order to eventually classify postures. Unprecise measurements would result in unclear force graphs and features for classification would be hard to determine. Precision is determined by the spread of the raw sensor output when the same load is applied multiple times. It can be expressed in terms of the percent deviation from the mean of the raw sensor output. An expression for the precision for each sensor is then:

$$Deviation_i = \left| \frac{S_i - \bar{S}}{\bar{S}} \right| \tag{3.4}$$

Where i indicates the measurement number, S is the raw sensor output, $\bar{S}$ the mean of the measurements and $Deviation_i$ the percentage deviation. To indicate the effect of load variation on precision, a test is executed with one sensor, one puck and a weight on top. The position of the weight is displaced from one side of the sensor to the other, within the boundaries that the center of mass of the weight is still above the puck. Raw sensor outputs values varied between a low reading of 1060 and a high reading of 1630. It should be noted that these low and high values were observed when the weight was placed near the opposing outer edges. This resulted in a sensor deviation of 21% around the mean.

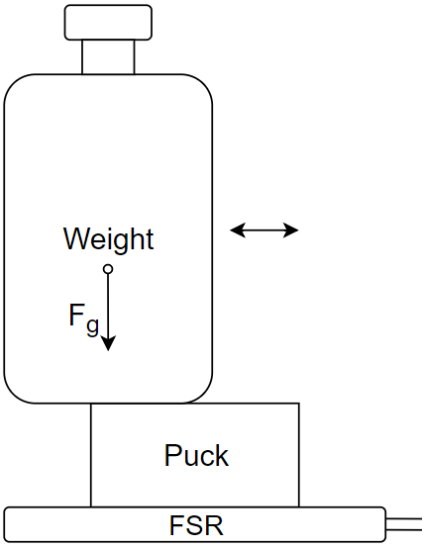

Figure 3.9: Weight displacement over the puck, from left to right, to measure the effect of different load distributions.

Calibrating and Determining Pressure Underneath the Mattress

To determine the correct force range of the sensor for the sensor system sensors, the pressure underneath the mattress was measured. A thin small scale was developed from available materials, seen in figure 3.10. It consisted out of four FSR's with pucks sandwiched between two discs of PMMA plate material. The area of the disks was 66mm, which due to the small area has the ability to measure localized pressure, yet it is not to small preventing high outlying pressure peaks. With a force reading from the FSR's the pressure could be determined from the known area.

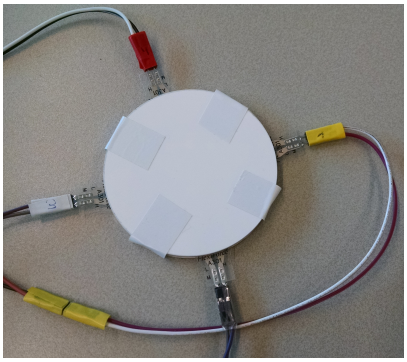

Figure 3.10: Sensor used to measure the pressure underneath the mattress

A relation between the sensor output and the applied load can be obtained by calibrating the sensors. Calibration can be achieved by relating the voltage output of the force to voltage circuit to a known force, in newtons. In terms of sensor errors the accuracy can then be defined as the range in which the calibrated sensor output deviates from true force applied.

Sensor accuracy is therefore dependent on calibration and the sensor specifications. For the Flexiforce sensors these properties are shown in table 3.1, according to the manufacturer. Effects that can be calibrated are the offset error, the slope error and the linearity error. It is chosen not to take the linearity error into account, since it is rated only 3% and requires a standardized and precise testing setup which to collect many reference data. Instead it is chosen to fit a first order polynomial curve on sensor outputs corresponding to known forces F applied on the sensor.

Force is applied by placing weights on the sensing area of the sensor. From the first order polynomial curve fit the slope error a and offset error are determined b, which can be used in post processing to relate the force to the raw sensorvalues according to:

$$F_{sensor} = \frac{Sensor_{out} - b}{a} \tag{3.5}$$

Table 3.1: Flexiforce sensor properties. Source [52]

Linearity (Error)	+/- 3%
Presicion	+/- 2.5% of full scale (conditioned sensor, 80% force applied)
Hysteresis	<4.5% of full scale (conditioned sensor, 80% force applied)
Drift	<5% per logarithmic time scale (constant load of 90% sensor rating)
Response Time	<5 microseconds

For the small scale the a and b factors are determined for four sensors with 50, 100, 200 and 500 gram load applied. Load is set applied for around 60 seconds, taken off for around 20 seconds and this procedure is repeated 10 times for each weight so the output can be averaged for one force reading.

To get an idea about the pressure underneath a mattress, a test is performed by varying the location of the scale underneath the mattress with a 88kg test person lying in a supine position.

The width of the mattress is 750mm, divided by the diameter of the scale 66mm this results in approximately 12 unique scale locations. The scale was placed between the four square holes of the bedframe. For every measurement the test subject moved from lying posture to a sitting posture so that the mattress could be lifted and the sensor be changed to the next location. This resulted in the following pressure graph:

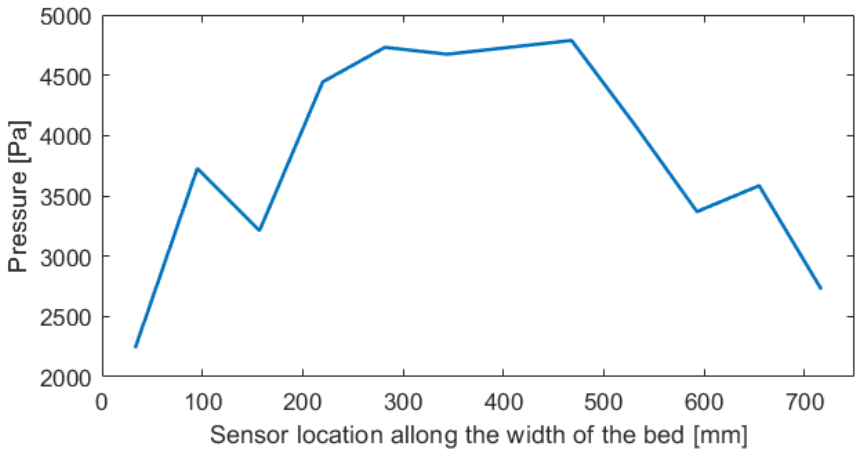

Figure 3.11: Pressure measured using the thin scale at twelve locations.

The pressure peaks at the side can probably be explained by a slight raise in the bedframe surface. Sensor locations 95 and 655 were right on the border of the raise in the bedframe and were slightly angled. FSR's measure the normal force and it is presumed that the mattress due to bending was more aligned to this angle so a higher pressure reading is obtained. A comparable effect is presumed for sensor locations 157 and 593, which were located right next to the raise in the bedframe, so that the bedframe took up part of this load. For a sensor system it is therefore desired to use a bottom plate covering the entire width of de bedframe to minimize this effect.

To have an indication about the maximum pressure that will occur underneath the mattress, the scale is placed in the middle and the pressure is compared for two test subjects laying in the middle of the bed in two postures. The outcome is shown in table 3.2, with 7742Pa as maximal pressure measured and it shows that pressure of the 90° side posture is higher than the pressure in the supine posture for both test subjects.

Table 3.2: Pressure values with the scale in the middle of the bedframe for supine and side 90° postures.

Test subject	**Weight [Kg]**	**Posture**	**Pressure [Pa]**
1	88	Supine	6595
1	88	Side	7742
2	65	Supine	4100
2	65	Side	5419

3.3.2 Sensor System Design Choices and Calculations

General design choices can be determined, based on the requirement analysed in the beginning of this chapter, together with the initial testing results. The initial testing showed that the way the load is distributed on the force sensing resistor has influence on the accuracy. A pressure capturing plate is proposed in several concepts and configurations. These were analysed and the best suitable setup was chosen. This setup is further analysed using an engineering optimization framework, to determine the dimensions of the plates. At the end the mechanical parameters of the sensor system are determined.

General Design Decisions

The sensor system should measure the most possible information with a low resolution sensor configuration. It is reasoned that measuring in the entire width of the bed would provide the best representation of the pressure curve underneath the mattress. This makes the maximal width of the sensor the width of the bedframe, which is 750mm.

To measure over the location of the holes in the bedframe, a bottomplate is needed. On this bottomplate an array of FSR's can be attached. This bottomplate should be rigid enough to provide resistance to bending at the locations of the holes in the bedframe.

The maximal total height of the sensor should be in range of 10mm. This leaves room for incorporating a bottom plate and the sensors, yet is thin enough not to be detected by a patient, which is verified during an experiment with one test subject using a piece of pate material of 10mm thick.

FSR's are sensitive to delamination when subjected to shear forces. These forces occur when the load vector on top of the sensor is not parallel with the normal force. Two joints are proposed which can constrain sideways sliding motion of the puck. These are a grooved sliding joint and a hinged joint. A hinge joint is difficult to fabricate when thickness is limited and in our application would also induce irregularities, since vertical load going through the hinge would not be measured by the FSR. A grooved sliding joint is chosen to be incorporated in the design since it is easy to construct on a thin scale and measures all the load above the sensor.

It is desired to measure all the load along the x axis and load which is taken up by the groove will not be measured by a sensor. Therefore this groove length l_g should remain small and the pressure capturing area should be higher than the groove height h_g. By making this area the highest part of the sensor, the pressure capturing surface is in direct contact with the mattress and the clearest signal will be measured.

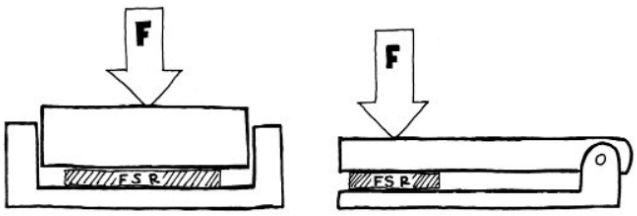

Figure 3.12: Joints for constraining shear forces: a grooved sliding joint (left) and a hinge joint (right), source [41].

Pressure Capturing Plates

A pressure capturing plate is proposed as a layer on top of the puck. Pucks have a small surface area and if they would be directly in contact with the mattress, they would only measure very small localized pressures peaks, which could induce irregularities in the force curve. It is therefore assumed that a larger sensing area would have a better result. Since a design goal is to limit the amount of sensors, a pressure capturing plate is proposed. Supported by pucks, a larger plate which is in contact with the mattress and captures the pressure underneath is way to increase the sensing area. Apart from increasing the pressure sensing area their secondary function is to constrain rotational movement.

During initial testing it has been found that the sensors are sensitive for unevenly distributed load above their pressure sensitive area. It is hypothesized that when a puck is loaded near its edge, that edge is compressed more due to the uneven load distribution. This causes that edge to compress more, inducing a very small rotation of the puck and a lower contact area where the majority force is supported. Since the compressed resistive polymer has irregularities in its production method, readings may vary for the same load if the puck is loaded near different edges.

To minimize this effect, a setup needs to be designed constraining the puck from rotation. To constrain rotation around two axes at least three support points are needed. Two concepts followed based on three and four puck support points, seen in figure 3.13 and these concepts can be placed in 3 configurations.

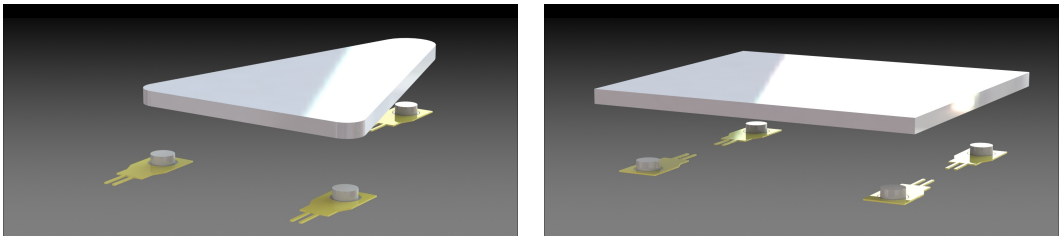

(a) Triangle shaped pressure capturing plate with 3 support pucks and FSR's in each corner.

(b) Rectangle shaped pressure capturing plate with 4 support pucks and FSR's in each corner.

Figure 3.13: Concepts for pressure capturing plates, with the plates raised from the pucks

A triangular concept as shown in figure 3.13a has three support points which provide the most stable surface. It can be set up in 2 array configurations: Universally oriented, seen in fig.3.14 (a) and alternating the orientation, seen in fig.3.14 (b). The rectangle shaped concept has a slight advantage over the triangle shaped concept. A rectangular array as shown in fig.3.14 (c), is symmetrical through the x and y centerline of the sensing area and its sensing area can cover the entire width of the mattress. Although a small difference, it is assumed that the rectangular concept will give a better representation of the force curve. It also provides the opportunity to calculate the center of pressure on the plate in both x direction as y direction.

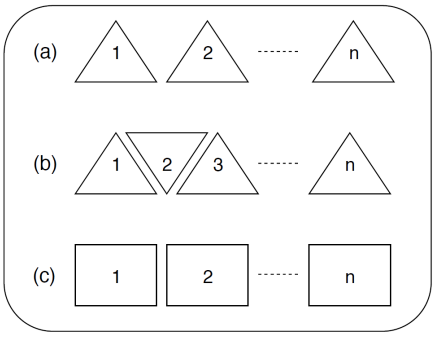

Figure 3.14: Plate array configurations.

Plate Material and Sensor Amount

In this section the material of the plate as well as dimensions length l, widht w and height h will be determined. The topview is illustrated in figure 3.15 and a cross section is illustrated in figure 3.16. Distance between the center of the pucks is given by l_{pp} and w_{pp} and the distance between the groove and the center of the puck is given by l_{gp} and w_{gp}.

It is not desired for the pressure capturing plate to have a large angular rotating caused by bending. This would cause an unevenly distributed load on the puck and the sensing area of the FSR, so the plate material should be stiff. Looking at the plate dimensions, it is mechanically determined that bending decreases when l and w decrease and h increases.

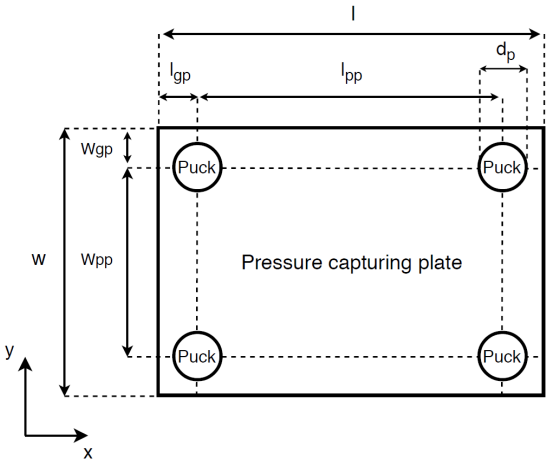

Figure 3.15: Top view displaying xy dimensions of the pressure capturing plate.

However there are some constraints if the requirements in section 3.1 are to be met. Since the total width of the bed is to be measured, decreasing l would result in an increasing amount of pressure capturing plates n_{plates}, resulting in more sensors to be used. This is better in terms of accuracy but undesirable due to the low cost requirement. Furthermore the height should be minimized according to the requirement of non-intrusiveness. This means a compromise between the stiffness, the amount of sensors and the height needs to be determined.

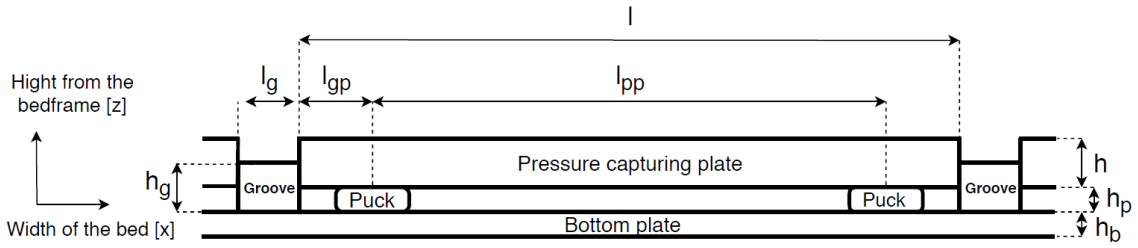

Figure 3.16: Cross section displaying dimensions in the xz plane of the pressure capturing plate.

Small offset distances between the centre of the pucks and the grooves (l_{gp} and w_{gp}) are proposed as a measure to lower the distance between the pucks for the same total length of a pressure capturing plate. This is possible as long as the center of pressure on the plate falls between the pucks. Since the mattress is assumed to gradually distribute the load of the patient, it is assumed that this will not be a problem as long as l_{gp} is smaller than l_{pp}.

The bending of the plate can be estimated by making some simplifications. First of all the pressure on top of the rectangle plate is assumed to be universally distributed. When analysing the plate in its profile seen in figure 3.16 and since it is already stated that $l_{gp} \ll l_{pp}$, the plate between the pucks can be simplified by a statically determined beam, with the precondition to this simplification that $l_{pp} > w_{pp}$ and the puck diameter neglected. The objective is to minimize the maximal angle caused by deflection:

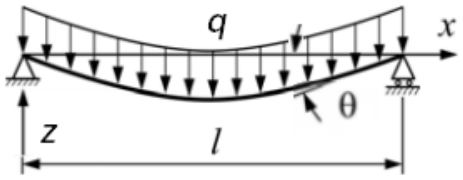

Figure 3.17: Supported beam with an evenly distributed load, source [15].

$$\theta_{max} = \frac{q l_{pp}^3}{24EI} \tag{3.6}$$

With the length l_{pp}, distributed load q, elastic modulus E and moment of inertia I. The elastic modulus is dependent on the material choice, the distributed load is determined by the pressure underneath the mattress induced by the patient and the length and inertia are determined by the plate dimensions. For the pressure underneath the mattress the highest loading scenario is then considered.

In the initial testing it was found that a person weighing 88kg could cause a pressure of 7742Pa in a side posture measured in the middle of the bed. However the sensor should be able to withstand the pressure of obese patient. Assuming a linear pressure increase for patient weight, a factor two of the measured pressure 7742Pa is assumed as a sufficient approximation of pressure caused by the weight of a 170kg patient. This means 15484Pa will be used as a parameter for maximal load in the following calculations.

At this point the material of the plate is chosen to be the polymer PMMA. This material is stiff compared to most polymers. Furthermore PMMA plate material is available in many dimensions, providing design flexibility and plate thickness up to 10mm can be processed fast within very small tolerances using a laser cutting machine. It is therefore considered more efficient in the production process compared to metals. This high tolerance is needed to obtain a close fit between the borders of the pressure capturing plates and the grooves in the encasing, yet without friction appearing in the borders.

Since the bottomplate also requires similar characteristics, PMMA will also be used there. For the remaining components PMMA will also be used, since the pucks need to be rigid, the bottomplate also requires similar characteristics as the pressure capturing plate and other framework like the grooves can easily be manufactured. 3mm plates will be used for the bottomplate and the pucks as it is assumed that they provide sufficient structure. The grooves will be formed by placing two 3mm plates on each other. The elastic modulus of PMMA is known as 2.8GPa.

Since it is desired to measure the load across the entire width of the bed (l_{bedx}), which is 750mm. This allows the number of plates in the array to be expressed in terms of the lengths of l_{gp}, l_{pp} and l_g. The amount of plates determines the amount of sensors ($n_{sensors} = 4 * n_{plates}$) and therefore need to be minimized according to the low cost requirement. In section 3.1, it reasoned that 5 sensing areas would be minimal for determining the skewness and kurtosis from the force signal, which can also be formulated an inequality constraint. These equations can be written as:

$$n_{plates} = \frac{l_{bedx} - l_g}{l_{pp} + 2l_{gp} + l_g} \tag{3.7}$$

$$n_{plates} \geq 5 \tag{3.8}$$

According to the non-intrusive requirement it is necessary to minimize the total thickness h_{tot} of the sensor. In the design choices it is reasoned that the pressure capturing plates have to be the highest part of the sensor to be in direct contact with the mattress. This means the total height of the plates is the sum of the heights of the bottom plate, the pucks and the pressure capturing plates, seen in equation 3.9. When rewriting equation 3.6, the height of the pressure capturing plate can be also expressed as a function of l_{pp} and θ_{max}. Since the pressure capturing plates h need to be the highest part of the sensor, the inequality constraint seen in equation 3.10 can be formulated. h_p and h_g are determined at 3 and 6mm respectively, meaning h should be higher than 3mm.

$$h_{tot} = h + h_p + h_b = \sqrt[3]{\frac{2Pl_{pp}^3}{E\theta_{max}}} + h_p + h_b \tag{3.9}$$

$$h > h_g - h_p \tag{3.10}$$

The ratio between l_{pp} and l_{gp} is named constant c. To keep the center of pressure between the pucks, l_{pp} over l_{gp} should be maximized. This can be formulated into an minimization objective by taking the negative of c:

$$-c = l_{pp}/l_{gp} \tag{3.11}$$

Summarizing the objectives above combined with their constraints, we get the minimization problem seen in equation 3.12 with four objectives, four variables and two constraints. Since there are more variables than constraints, this is an underdetermined problem with a 4D solution space.

$$\begin{gathered} \min(N_{plates}(l_{gp}, l_{pp}), H_{tot}(\theta_{max}, l_{pp}), -C(l_{pp}, l_{gp}), \Theta_{max}(h, l_{pp})) \\ s.t. \\ n_{plates} \geq 5 \\ h > 3 \end{gathered} \tag{3.12}$$

By taking for example n_{plates} at the minimum of 5, the 3D solution space can visualized with Matlab by calculating the variables h, c and θ_{max} for a variation of c and h. This gives an indication about the sensitivity of the variables. For example it can be seen that varying h has the more impact on θ_{max} compared to c, because if h decreases, θ_{max} rises exponentially where h seems to behave as a horizontal asymptote.

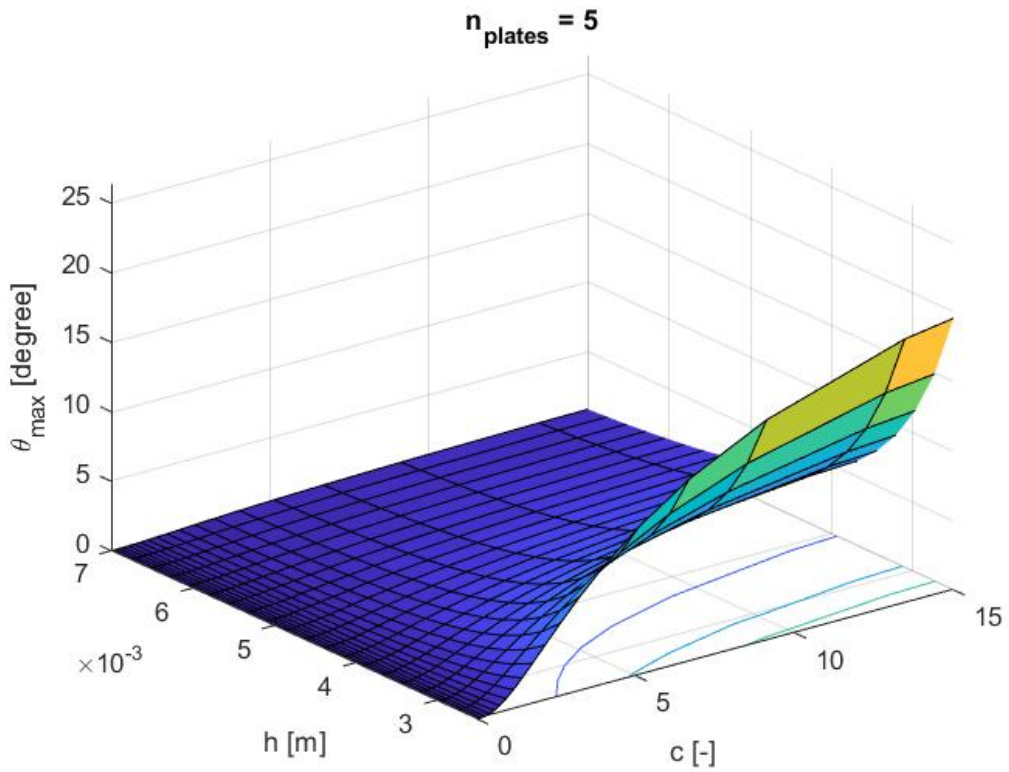

Figure 3.18: Solution space for variables h, c and θ_{max} if $n_{plates} = 5$

Limiting the solution space is possible by adding constraints. Since the deflection is required to be low, the maximum angle of deflection will be specified as 1 degrees and a ratio c of 7 is assumed to fulfil $l_{gp} \ll l_{pp}$ since we expect a gradual distribution of pressure underneath the mattress. Specifying the minimization functions for c and θ as inequality constraints, the following optimization problem:

$$\begin{aligned} &\min(N_{plates}(l_{gp},l_{pp}), H_{tot}(\theta_{max}, l_{pp})) \\ &s.t. \\ n_{plates} &\geq 5 \\ h &> 3 \\ c &\geq 7 \\ \theta_{max} &\geq 1 \end{aligned} \tag{3.13}$$

Having still two minimization objectives a compromise still needs to be made between the height and the number of plates. h_{tot} varies only with different height of the pressure capturing plates, since the bottomplate and puck height are already defined, so h is used in further analysis. The

height and number of plates vary in discrete integer steps and an overview is created in figure 3.19 where $n_{plates} = [5,6,7]$ and $h = [4,5,6]$ can be compared. The constraints have been plotted as a full line and the dotted line indicates the side of the constraint line that is not eligible for a solution.

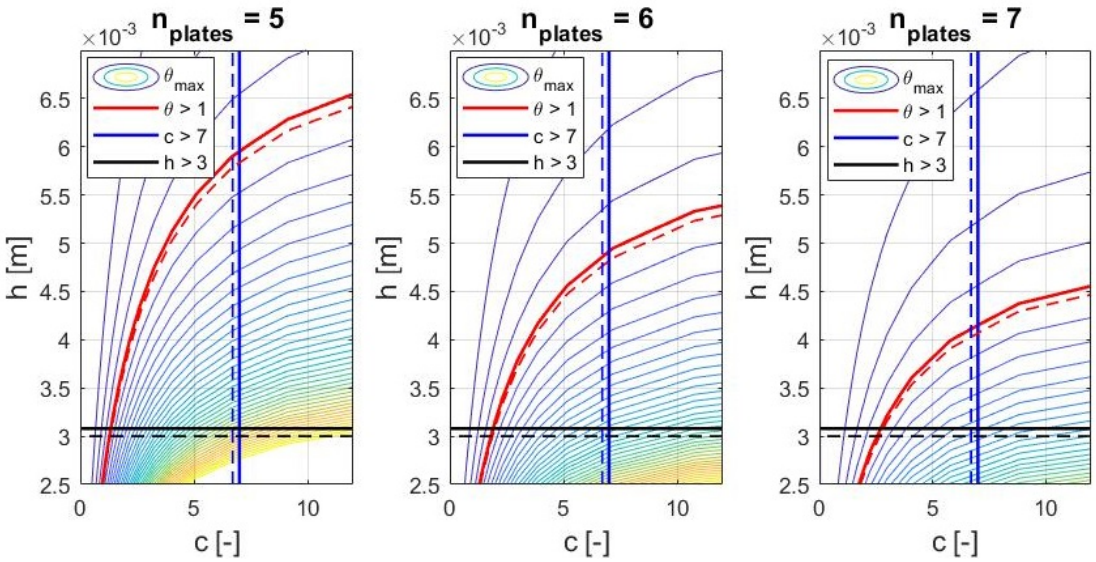

Figure 3.19: Contour plots depicting the solution space for equation 3.13, comparing the height and the number of plates. The contour lines indicate the solution space for θ_{max}, the solid lines indicate the constraint barriers and the dotted lines indicate the sides that don't fulfil the constraints.

For $n_{plates} = 5$ there is no solution as the angle at the heighest height of 6mm falls just outside the constraint threshold. In case $n_{plates} = 7$ we see the same for the height of 4mm, so here a height of 5mm would be the most optimal option. However for $n_{plates} = 6$ the height of 5mm is right on the threshold boundary and still a feasible solution. Since we want to minimize both, $n_{plates} = 6$ with $h = 5$ is chosen as the most optimal compromise.

This setup fulfils both the non-intrusive requirement as well as the cost requirement since there are only 24 sensors with $n_{plates} = 6$ and is assumed to measure the force underneath the mattress with sufficient resolution to determine skewness and kurtosis. These values can be used to calculate the remaining parameters according to the previous equations to determine the other parameters. This results in the following design parameters listed in table 3.3:

Table 3.3: Dimensions used in the final design.

Parameter	Value	Unit
l_{pp}	90	mm
l_{gp}	12.5	mm
l_g	7	mm
d_p	8	mm
w_{pp}	75	mm
w_{gp}	12.5	mm

3.3.3 Final Sensor System design

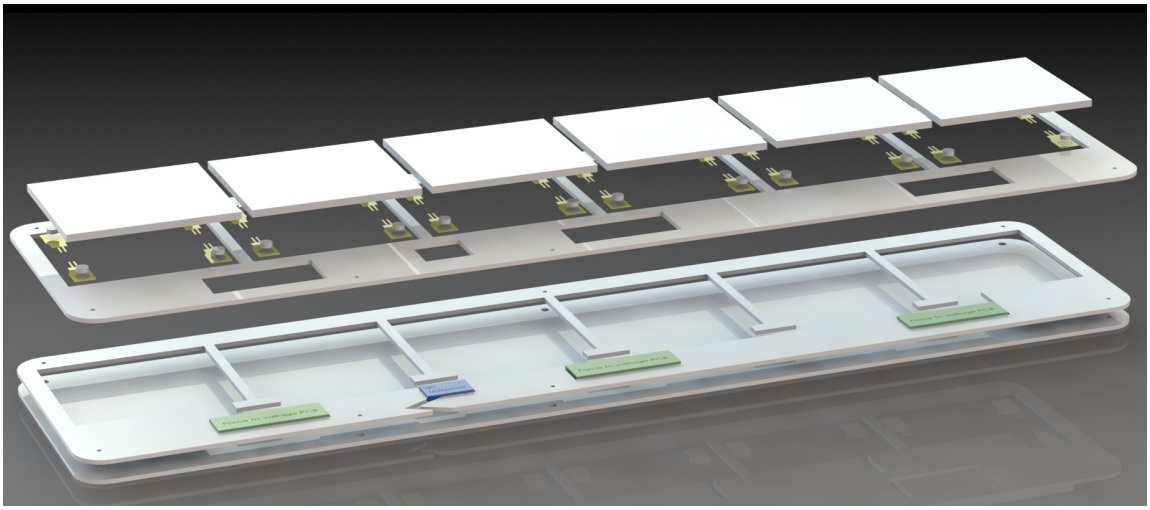

Figure 3.20: Exploded view illustrating the different plate layers of the sensor system.

With a rectangular plate as a sensor design and the design parameters determined by the optimization analysis, Solidworks is used to model the final sensor system which will be used for the experiments. An exploded view is illustrated in figure 3.20, showing the plate layers, the sensors, the pucks and the electronics, with the force-to-voltage printed ciruit boards (PCB's) shown in green and a multiplexer shown in purple. The total outer dimensions are 200x750x11mm.

With six pressure capturing plates, there are 24 force sensing resistors used in the sensor system. Following the design parameters calculated in table 3.3, the pressure capturing plates have a total length and width of 115mm and 100mm, the surface area of the plates is 115cm^2. With an estimated maximal pressure of 15484Pa, the maximum force on a plate is calculated as 178N. Since this force is supported by four FSR's, the Flexiforce sensors with force range of 110N are chosen to be incorporated in the design.

The company Momo Medical provided three small PCB's which can be used to readout eight FSR's each, with a comparable analogue circuit as used in the initial testing. This allowed the implementation of the force-to-voltage circuit inside the sensor and close to the sensors, which made it possible to limit the total cable length.

The ADC's in the PCB's can communicate the raw sensor values to a processing unit using the I^2C communication protocol. The I^2C communication protocol allows a "master" device to communicate with multiple "slave" integrated circuits. The master device, which is in this case a raspberry pi, can readout multiple slave devices if they have a different address. Unfortunately the amount of address options that can be setup with the ADC's used here are 4 and there are 6 needed. This requires an I^2C multiplexer that can sample the data from multiple devices with the same address.

A sampling time of 2Hz is determined since the objective is to compare snapshots of the force curve with each other and not looking at the rate of change. Furthermore the signal to be measured is not expected to change fast in time.

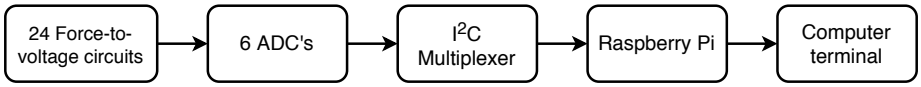

Figure 3.21: Overview of the information flow from the sensors to the computer terminal.

The sensor system was manufactured by lasercutting PMMA plates, wiring the sensors and connecting each sensor to the force-to-voltage PCB's. The force-to-voltage PCB's are wired to the I^2C multiplexer and a long wire connection has been made between the multiplexer and the raspberry pi. The bottom plate and the spacer plate are connected with double sided tape. The two lower plates are held together with the top plate by bolts.

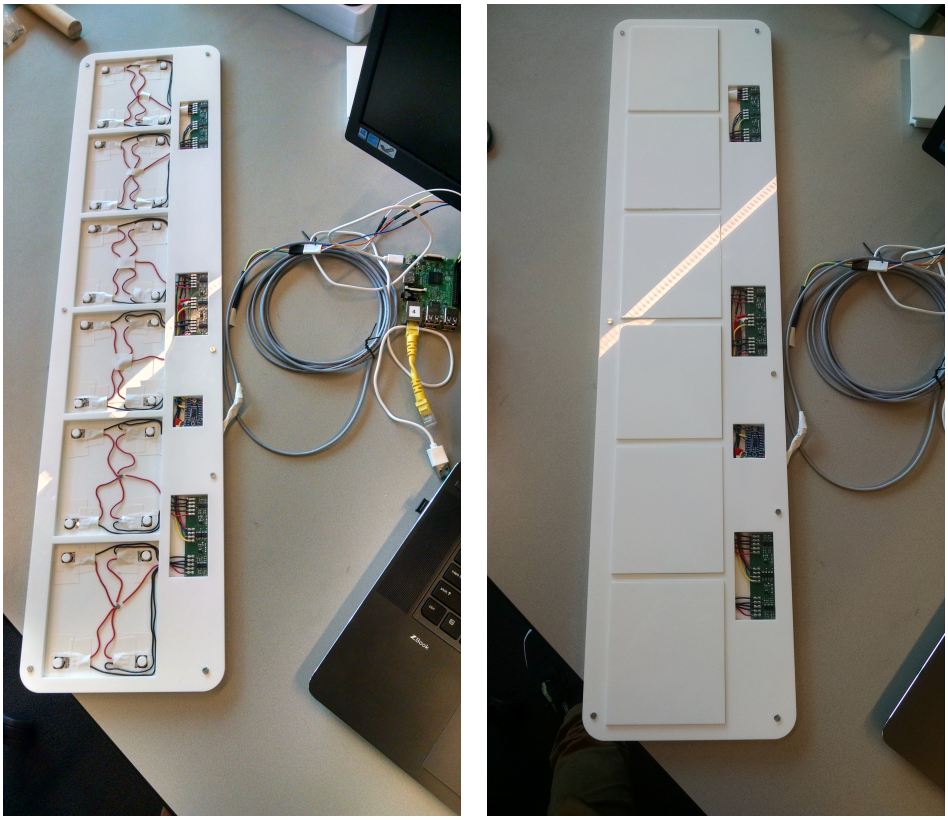

(a) Without pressure capturing plates. (b) With pressure capturing plates.

Figure 3.22: Manufactured sensor system.

Sensor System FSR Calibration

Calibration is performed comparable to calibrating the small scale in section 3.3.1. Since it was found that the precision is affected by the consistency of the load path on the sensor it is chosen to calibrate the sensors within the surrounding encasing. This is done by placing weights on top of the pressure capturing plates with the aim of placing the weight directly above the sensor, ensuring the load path to go through the sensor we want to calibrate. The location of each sensor is marked above the plate to ensure correct placement. Since precision is an important factor with these sensors, every measurement is executed 3 times for each weight. To ensure that the sensor is properly settled a measuring time of one minute is taken. After approximately 20 seconds of measuring the value is averaged to obtain the raw value for that measurement.

Two weights were used. A standardized 500g weight and a dumbbell weight. Since it was difficult to place the dumbbell weight precisely, a custom build guiding mechanism was used. This arm allowed normal force to go through a puck placed on the bottom and constrained the remaining degrees of freedom. The weight of the dumbbell was 1317 gram but since a small amount of load went through the support of the arm and it having a small mass itself, a reference measurement of the guiding mechanisms with the weight is taken using a scale, reading a weight of 1364 gram.

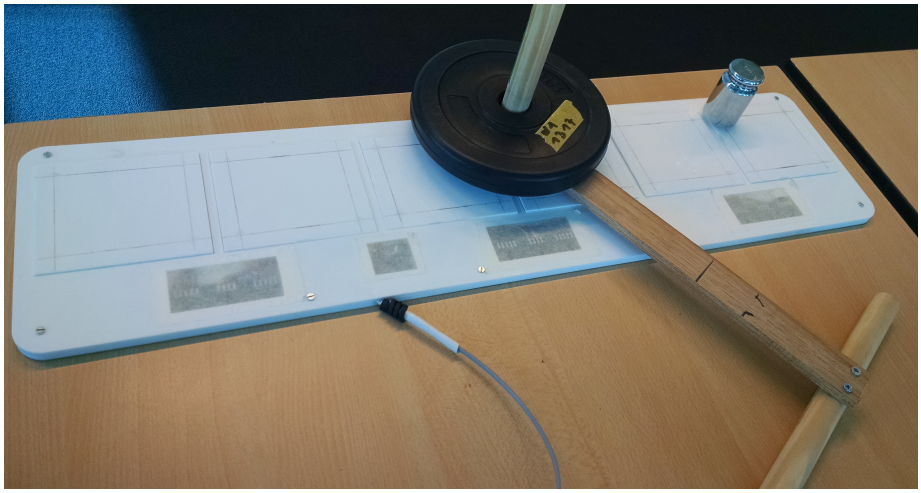

Figure 3.23: Calibration using a 500 gram weight and a 1317 gram dumbbell weight in combination with a weight guiding system.

With the sensor output for each measurement a polynomial fit can be obtained according to equation 3.5, resulting in an a and b value for each sensor. To visualize the sensor behaviour, the raw sensor output is plotted against the force applied in figure 3.24.

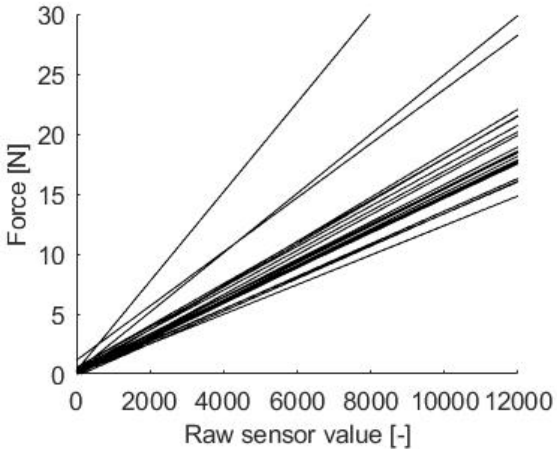

Figure 3.24: First order polynomial fit plotted for each sensor. It can be seen that most of the sensors have a similar slope, with a few significant outliers.

For six datapoints measured per sensor, the percentage of sensor output deviation from the mean is calculated by equation 3.4 as an expression for the precision. It has the purpose to check the performance of calibrating within the encasing. The precision per sensor is given in a boxplot in figure 3.25, with an overall mean deviation from the sensor measurements of 2.57%.

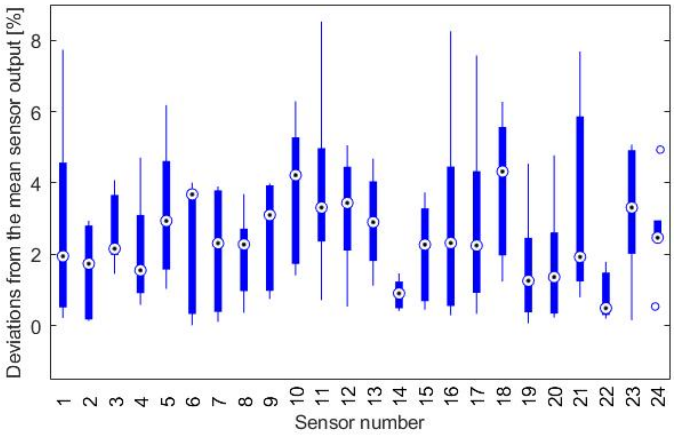

Figure 3.25: Box plot giving the percentage of sensor output deviation from its mean, for the measurements obtained during the calibration procedure.

3.4 Patient Bed Posture Classification

The sensor developed in section 3.3 only measuring pressure distribution underneath the mattress, so the majority of parameters of the system, being a patient on top of a mattress, are not known. Patients vary in weight, height and body type, in addition the lying position in bed, rotation of the chest and arm and leg placements could all vary for the same posture. Furthermore there are differences in mattress types and material properties. Even if the system is simplified enough so that a generic model of how posture pressure propagates through the mattress is made, it would probably not be useful in practice for posture identification purposes.

Therefore it is proposed to use machine learning for the posture identification task. This approach is more robust with high system variability, as it tries to find the best possible correlations in the limited information available, for making a new prediction. In general, machine learning uses reference data to produce a program that can perform a task. The reference data is provided by the sensor system for which the postures can be observed during an experiment. The program is a predictive model for which both input as the force curve and output data as the postures are known. Since both input and outputs are known, supervised learning techniques could be used to train the predictive model, in the category classification algorithms since posture outputs are discrete. In order to train the classification model the following steps were taken:

- Dataset creation trough two experiments
- Preprocessing data
- Classification algorithm development

3.4.1 Experiment protocols

Two experiments were conducted, in which test subjects were asked to lie in different postures in a standard Hill-Rom Hospital bed, with the amount of postures equally balanced. With the purpose to be clinically implementable for pressure ulcer prevention, it is the goal that the sensor system is compatible with current pressure ulcer prevention strategies. In the background on section 2.3 there were two main strategies identified. These are the use of specialized support surfaces and the use of five repositioning postures: left lateral -90°, left lateral -30°, supine 0°, right lateral 30°and right lateral 90°.

The first experiment was designed to analyse the hypothesized features in the force curve. In order to make a robust classification model the force curves and the calculated features should be repeatable for a person lying multiple times in the same posture. Two people are included in this experiment for reference and measured multiple times at the most common postures: left -90°, supine and right 90°. This experiment was performed on both a foam and air mattress so their feature spaces could be compared.

The second experiment has the purpose to create a dataset to develop and grade a classification algorithm for multiple test subjects for the five postures relevant for repositioning. With these objectives, two experiment protocols are proposed:

Figure 3.26: Sensor system location was secured using tape.

1. Experiment one: Foam mattress compared to an alternating air mattress.
   (a) Two test subjects
   (b) Three postures: Left -90°, Supine, Right 90°
   (c) Six times in/out bed
2. Experiment two: Comparing five repositioning postures for several test subjects.
   (a) 22 test subjects
   (b) Five postures: Left -90°, Left -30°, Supine, Right 30°, Right 90°
   (c) Two times in/out bed per subject

For the lateral 30°posture a wig shaped back cushion is used, as seen in figure 2.6. A sequence of postures is performed which are measured for one minute each. The only instruction that is given to the test subjects apart from the posture is to lay approximately in the middle of the bed. The subject is free to choose arm and leg positions as this is also an uncontrollable factor in a hospital environment. The in/out bed procedure is proposed to get a subsequent reading for the test subject, which is also done for one minute. The order of postures is randomised to exclude covariance of the posture order.

Since this is a pilot study to assess the feasibility of posture detection using a sensor system underneath the mattress, it is not yet needed to perform the experiment with test subjects sensitive for pressure ulcer development. From these test subjects the information that is gathered is the weight, length and their gender. The above protocol was approved by the TU Delft Human Research Ethics Committee.

3.4.2 Preprocessing Data

Using all sensor data as an input would result in an inefficient classification algorithm with high processing time. To reduce this processing time it is chosen to express the relevant signal data into three features. These features are based on the hypothesis formulated in the beginning of this chapter, with as an addition the location of the mean of the force distribution.

The data from the experiments are gathered and afterwards processed offline using Matlab. During the experiments the data is saved in a comma separated text file and imported into Matlab as a matrix with the 24 sensor values for each sample. First the labelsamples corresponding to each posture are determined. Since there were slight variations in the exact timing during each test, this had to be done manually. The labelled data points for the second experiment can be seen in appendix A. The data file was assessed and the sample corresponding to the posture sequence were noted. For these samples the following processing steps are proposed:

1. Calibrating each sensor
2. Calculating center of pressure in x direction (CoP_x) for each plate
3. Determining the force graph over the x direction of the bed
   (a) Adding the forces over each plate to get six data points
   (b) Normalization of the forces

(c) Forming the force graph from the normalized forces and corresponding CoP_x

4. Simulating the force curve as a probability distribution

5. Calculating skewness, kurtosis and mean of the force probability distribution

Calibration is performed by relating the measured voltage to known force using the a and b values corresponding to each sensor value. The other processing are explained in the following subsections.

Calculating Center of Pressure and Normalization

The center of pressure in x direction can be calculated by the weight of each sensor in relation to the distance in between the sensors. If the left side of the sensor system is taken as a reference point, starting with sensor 1, then a ratio between the right two sensors and the total weight on the pressure capturing plate can be calculated. Multiplying this ratio with the length between the left and right sensors (l_{pp}), the center of pressure in x direction is obtained. Adding this to the location of the left two sensors of the n^{th} plate, the location of the center of pressure for the n^{th} plate is determined:

$$l_{CoPx_n} = l_{sL_n} + l_{pp}\frac{\bar{s}_R}{\bar{s}_n} \tag{3.14}$$

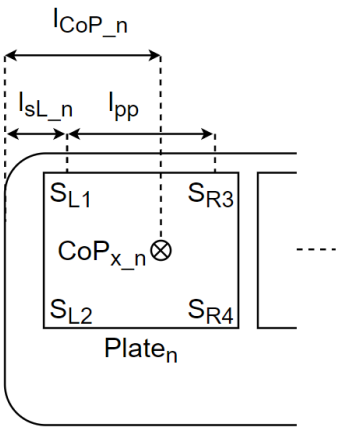

Figure 3.27: Distances for the center of pressure calculation.

Normalization of the force curve is proposed as a measure to minimize the effect of weight differences between test subjects. This normalization is obtained by dividing each data point of the force curve by the sum of all the force data points.

$$Fnorm_i = \frac{F_i}{\sum_{i=1}^{n} F_i} \tag{3.15}$$

Calculation of the Skewness, Kurtosis and Mean of the Pressure Distribution

The skewness, kurtosis and normalization of the force curve was based on the method proposed by Hsia et al. (2008) [24]. The difference with the method described here is that instead of having the sensor on the x axis of the force curve, the location of each CoP_x is considered and that the mean of the distribution will also be added as a feature. By calculating the CoP_x of each plate and relating it to the force measured on a pressure capturing plate an improved representation of the force curve underneath the bed can be obtained.

In probability theory, the skewness and kurtosis are measures of characteristics about a probability distribution. To calculate them for the measured force curve, it is necessary to consider the force curve as the probability distribution. The force curve consists out of 6 discrete force data points with on the x axis their location of the force on the sensor system and on the y axis the normalized force for each data point. Since the data points are discrete, the force curve can be considered as a probability mass function, with as possible outcomes (sample space S) the locations of the data points on the sensor system. Each of the discrete force locations have a probability which corresponds to the normalized force value for that location. This value represents the probability P that a "randomly discrete force location" will be a "certain discrete force location".

To comply with the formulas that calculate skewness and kurtosis of a probability mass function, a sample size is needed. For a simulated experiment, the simulated sample size is total amount of events and the sample set a set containing the outcome for each event. The amount that each outcome occurs in the sample set is determined by the probability for that discrete outcome in the probability mass function.

For example during the post processing of the experiments a simulation size of 10,000 is considered. For a certain force curve the first force is measured at location 76mm with a probability 0.145 and the second force is measured at location 191mm with probability 0.171. The sample vector then would contain 1450 samples with value 76 and 1710 samples with value 191. The following values in the sample vector are determined by the remaining location values and their corresponding probabilities.

From this sample vector the mean, skewness and kurtosis can be determined. The mean of the simulated distribution is the sum of all the samples divided by the total number of samples. Since the simulated probability distribution is a representation of the force distributed across the sensor, the result can be seen as the location of the average pressure. Skewness is defined as a measure of asymmetry of data around a sample mean. The sample skewness is calculated as follows:

$$s = \frac{\sqrt{n(n-1)}}{n-2} \sum_{i=1}^{n} \left(\frac{x_i - \bar{x}}{\sigma} \right)^3 \tag{3.16}$$

With σ the sample standard deviation, n the sample size and $\bar{x}$ the sample mean. The kurtosis is defined as a measure of the amount of outliers, in other words a measure of the "flatness" of the tails of the probability mass function. It is calculated as follows:

$$k = \frac{(n-1)n}{(n-2)(n-3)} \sum_{i=1}^{n} \left(\frac{x_i - \bar{x}}{\sigma} \right)^4 - \frac{3(n+1)^2}{(n-2)(n-3)} \tag{3.17}$$

3.4.3 Classification algorithm development

The experiment provided a labelled dataset for which features were calculated. This dataset was used to develop a classification algorithm, for which there were three main steps: training different machine learning algorithms, optimizing their parameters and testing the accuracy at the end.

To test the accuracy it is necessary to divide the data into a test set and a training set of 20% and 80% rounded respectively. To reduce influence of overfitting to patients, it is chosen to make a test set based on excluding four patients rather than taking that percentage of the all the datapoints combined. Testing the algorithm on data coming from patients who were not used in the training phase would give the best representation of the application of this technology.

Two common machine learning algorithms were considered based on usage in previous posture classification literature. These are support vector machines (SVM) and k-nearest neighbours (KNN). Using the Matlab classification toolbox, the algorithms were trained and parameters are optimized on their performance through 10 fold cross validation. The best performing algorithm was chosen to be used for evaluation on the test set.

K-Nearest Neighbours The k-nearest neighbour algorithm is a classification method where the class of a new data point is equal to the majority of k closest training samples calculated with the Euclidean distance, where k is a positive integer. Given the three feature space, determined by the skewness, kurtosis and mean of the distribution, in a Cartesian coordinate system, the Euclidean distance between a known point in the training set p and a new point in the testing set q is:

$$d(\boldsymbol{p}, \boldsymbol{q}) = \sqrt{(p_1 - q_1) + (p_2 - q_2) + (p_3 - q_3)} \tag{3.18}$$

Figure 3.28 shows how choosing k can determine the accuracy for a newly classified point. Given the test dataset which has labelled data, the optimal value for k is iteratively determined by evaluating the cross-validation accuracy for several values of k and choosing k with the highest accuracy.

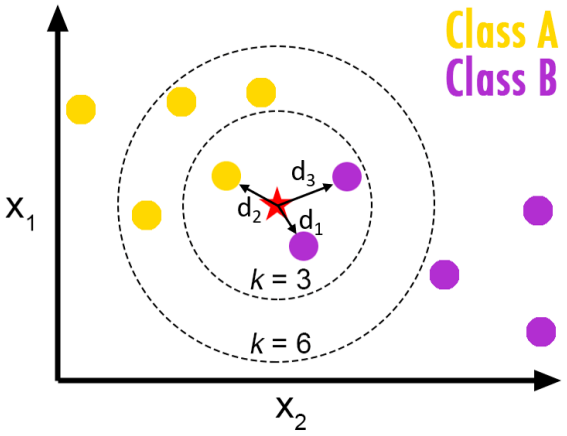

Figure 3.28: KNN algorithm visualization for two classes (A,B) in feature space (x_1,x_2). A new data point gets classified by calculating the nearest k data points through their Euclidean distance, source [13].

Support Vector Machines A SVM is a binary linear classifier which constructs $n-1$ dimensional maximal-margin hyperplanes in the R^n feature space, which work as decision boundary between classes. For two classes y_i, the decision hyperplane trained on of linearly separable data x_i is given by:

$$f(x) = \boldsymbol{\omega}^T \boldsymbol{x} + b = 0 \tag{3.19}$$

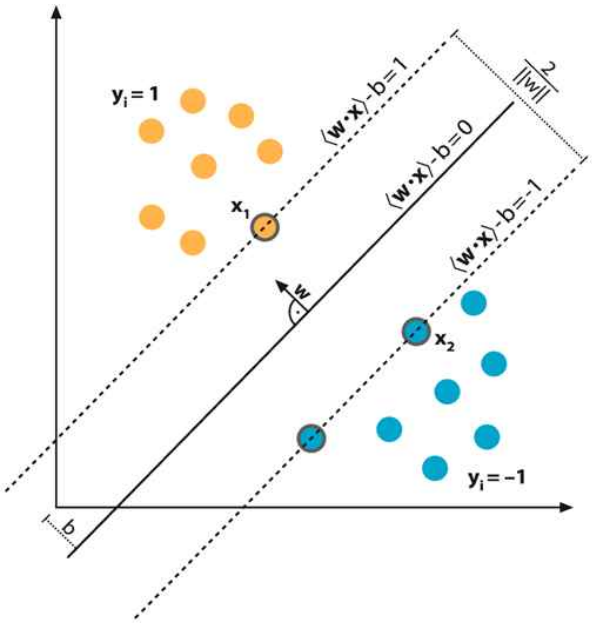

Figure 3.29: SVM algorithm visualization for two classes (1,-1) in a 2D feature space. A new data point gets classified by calculating the distance from the hyperplane, source [1].

Where the class for a new data point x is given by the sign of $f(x)$, $\boldsymbol{\omega}$ has the same dimension as the data x_i and b is a real number. The best separating hyperplane is given by the maximal margin width between the two classes, which is given by $\frac{2}{||\boldsymbol{\omega}||}$, such that $y_i f(x_i) \geq 1$, where $y_i = \pm 1$. The support vectors are located on the boundary where $y_i f(x_i) = 1$.

For mathematical convenience it is often represented as an optimization problem of minimizing $||\boldsymbol{\omega}||$ dependent on $\boldsymbol{\omega}$ and b. It can be calculated following the duality principals from optimization theory, using Lagrange multipliers. The primal optimization function is the minimization of the objective function subtracted from the constraints multiplied by Lagrange multipiers α_i.

$$\min L_P = \frac{1}{2}||\boldsymbol{\omega}||^2 - \sum_{i=1}^{n} \alpha_i \big[y_i(\boldsymbol{\omega}^T \boldsymbol{x}_i + b) - 1 \big] \tag{3.20}$$

The minima is reached at the point where the partial derivatives for $\boldsymbol{\omega}$ and b are zero. Taking the partial derivative for those result in the constraints 3.21, 3.22 and in the duality function 3.23.

$$\boldsymbol{\omega} = \sum_{i=1}^{n} \alpha_i y_i \boldsymbol{x}_i \tag{3.21}$$

$$0 = \sum_{i=1}^{n} \alpha_i y_i \tag{3.22}$$

$$\max L_D = \sum_{i=1}^{n} \alpha_i - \frac{1}{2} \sum_{i=1}^{n} \sum_{j=1}^{n} \alpha_i \alpha_j y_i y_j \boldsymbol{x}_i^T \boldsymbol{x}_j \tag{3.23}$$

Where the nonzero α_i in the solution for the duality function determine the margin as support vectors. The decision boundary is obtained by substituting $\boldsymbol{\omega}$ in equation 3.19 by the relation found for $\boldsymbol{\omega}$ in equation 3.21. For non-linear separable input data a kernel functions can be used to map the input data to a higher dimensional feature space.

$$K(\boldsymbol{x}_i, \boldsymbol{x}_j) = \phi(\boldsymbol{x}_i) \cdot \phi(\boldsymbol{x}_j) \tag{3.24}$$

For non-separable data the margin can be determined to separate most of the data points, also noted as a soft margin. This is induced by adding a slack variable ξ and regularisation parameter C. The optimization problem then becomes the problem listed in equitation 3.25 and can also be solved according to the duality principle using Lagrange multipliers.

$$\begin{gathered} \min \left(\frac{1}{2} ||\boldsymbol{\omega}||^2 + C \sum_{i=1}^{n} \xi_i \right) \\ s.t. \\ y_i(\boldsymbol{\omega}^T \boldsymbol{x}_i + b) \geq 1 - \xi_i \end{gathered} \tag{3.25}$$

Chapter 4

Results

4.1 Experiment One: Foam mattress compared to an alternating air mattress.

The force graph of two test subject are compared in this experiment, who perform an in/out bed protocol six times for each mattress type. Data is gathered according to the experiment protocol in section 3.4.1. The demographics of the two test subjects are given in table 4.1.

Table 4.1: Subject demographics for the first experiment.

Subject	Weight [kg]	Length [m]	Gender
1	67	173	M
2	57	163	F

After execution of the experiment the data was assessed. Figure 4.1 shows the sum of the raw sensor outputs per pressure capturing plate on the y axis, plotted against the duration time of the experiment on the x axis. Next the timestamps corresponding to the posture protocol were selected. They are indicated in the figure by the vertical dotted lines.

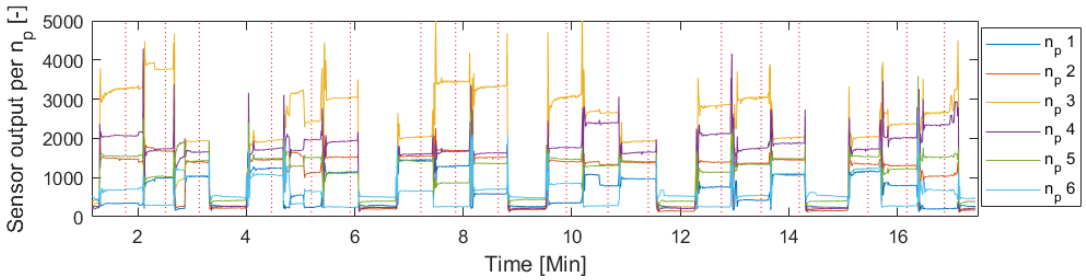

Figure 4.1: The force measured on six pressure capturing plates (n_p) plotted in time, for subject one on a foam mattress. Where the force on a pressure capturing plate is equal to the sum of the four raw sensor values.

The labelsample selection was performed for each of the four test series. The result is a dataset of 72 force curves, which are separated into 12 curves for each posture and mattress type. The force curve for the posture on the foam mattress is plotted of each test subject in figure 4.2 to visualize the repeatability of the curve per posture.

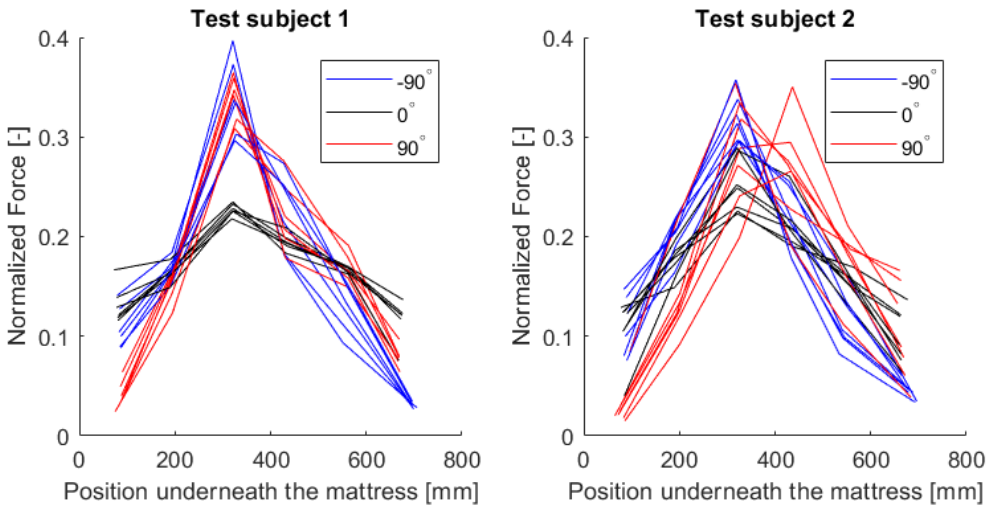

Figure 4.2: Force curves comparison between the two test subjects underneath a foam mattress.

The effect of the mattress on the force curve are visualized plotting the force curves of the two test subjects in a graph for the foam and air mattress, shown in figure 4.3.

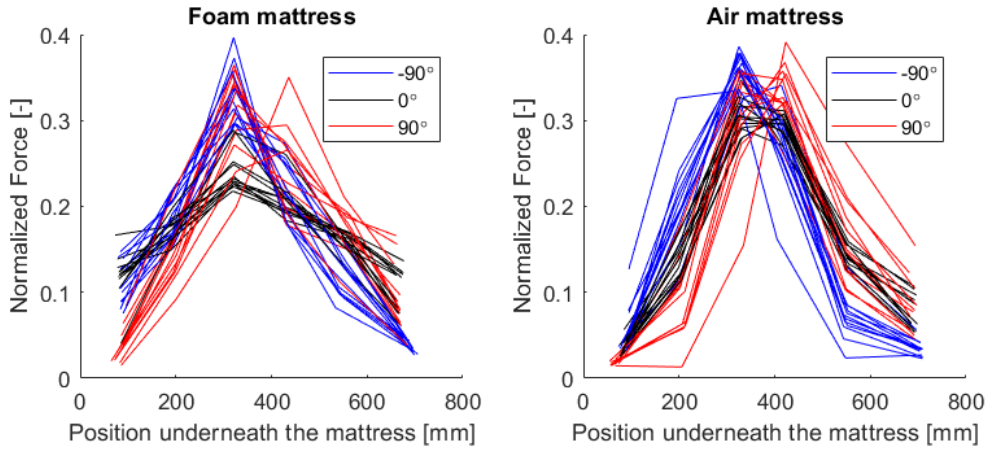

Figure 4.3: Force curves for test subject 1 and 2 for the postures supine 0° , left lateral -90° and right lateral 90° , measured on the foam and air mattress.

For a better comparison of the air and foam mattress, the force curves are averaged per posture in figure 4.4. Here some similarities can be identified when comparing the force curves per mattress.

The left -90° and right 90° postures have an opposite skew for both mattresses. It can be seen that for both the foam and the air mattress, the supine postures have a lower ratio of the maximum force over minimum force than the side postures, indicated by a lower kurtosis. Lastly it can be seen that the air mattress has an overall higher kurtosis than the foam mattress, for all postures.

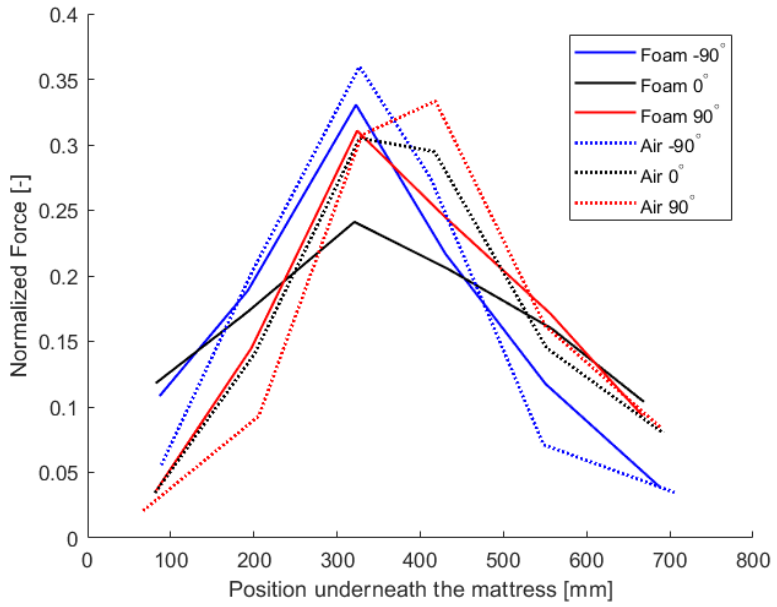

Figure 4.4: Force curves averaged per posture for the air and foam mattress.

The skewness and kurtosis can be calculated as described in 3.4.2. The scatterplot in figure 4.5 shows similar characteristics in skewness and kurtosis as seen on the averaged force curves, which is promising result for their use as features for classification. Cluster characteristics are seen the most for the supine posture. An opposite skewness is seen for left and right lateral posture clusters with the supine posture cluster being centered between the two. Furthermore the kurtosis for the supine posture on each mattress type is lower than the kurtosis for the side postures on the same mattress.

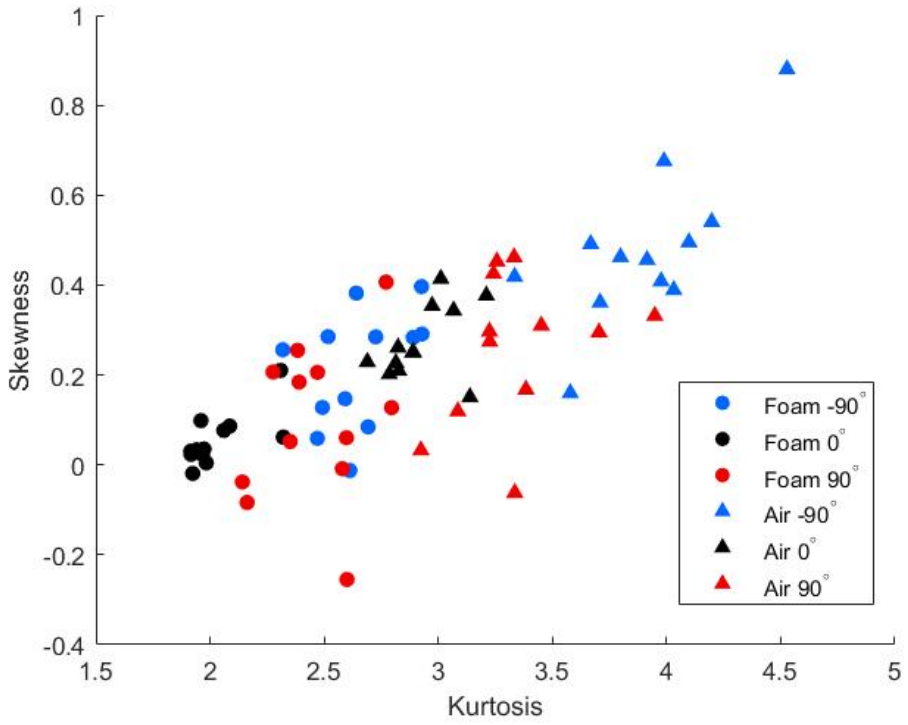

Figure 4.5: Skewness and kurtosis feature space for two test subjecs on the foam and air mattress.

From figure 4.5 can be seen that there is a good indication for the use skewness and kurtosis as features in a posture classification algorithm. However it will be necessary to make a classifier for each mattress type separately, since the clusters of the postures for the air mattress appear to be a scaled version of the cluster for the foam mattress.

4.2 Experiment Two: Classification of Three and Five Postures

In the second experiment multiple test subjects are included to perform an in/out bed protocol two times on a foam mattress. First the force curve for all the test subjects are observed, after which the data is divided into the train and test set to develop and evaluate a classification algorithm.

Twenty two healthy young adults were included in the second experiment, of which 68% were male. Demographics for all test subjects are given in table 4.2 with a mean weight, length and BMI of 1.795 meter, 75.6 kg and 23.3 respectively. Excluding the test subject datasets with missing data points due to a readout inconsistency, subjects 9, 11, 12, and 18 are randomly selected as the test set.

Table 4.2: Subject demographics for the second experiment.

Subject	**Length [m]**	**Weight [kg]**	**BMI**	**Gender**
1	1.84	83	24.5	F
2	1.73	58	19.4	F
3	1.86	74	21.4	M
4	1.82	90	27.2	M
5	1.81	78	23.8	M
6	1.64	54	20.1	F
7	1.72	67	22.6	M
8	1.76	89	28.7	M
9	1.63	57	21.5	F
10	1.68	57	20.2	F
11	1.83	88	26.3	M
12	1.76	75	24.2	M
13	1.91	93	25.5	M
14	1.73	65	21.7	F
15	1.7	70	24.2	F
16	1.88	82	23.2	M
17	1.88	87	24.6	M
18	1.92	80	21.7	M
19	1.8	80	24.7	M
20	1.83	82	24.5	M
21	1.95	85	22.4	M
22	1.81	70	21.4	M
Mean	1.795	75.6	23.3	

After the execution of the second experiment the timestamps were selected in the same manner as described in section 4.1. Force curve for all the test subjects were randomly selected and visualize the generalized differences in the force curves for each posture, the force curves for each posture are averaged for all the test subjects and given in figure 4.6. It shows similar patterns compared to the figure 4.4, however the 30° postures are skewed opposite to the 90°postures. This is presumably caused by the back cushion used for the 30°posture which spreads the back pressure on the mattress, resulting in less force to be measured at the sensor system location. Generally the 30° posture causes

the location of the shoulder in contact with the mattress to be on the opposite side measured from the centerline of the bed compared to the 90° , resulting in an opposing skewness.

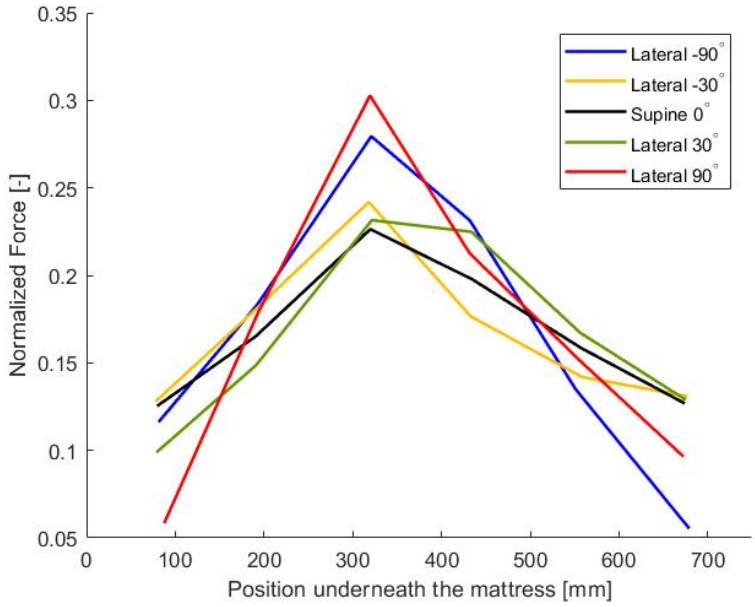

Figure 4.6: Normalized force curves averaged per posture, for the 18 test subjects in the training dataset.

The force curves for the training set are pre-processed into three features: skewness, kurtosis and the mean of the simulated pressure distribution. The 3D feature space is visualized by two 2D scatter plots in figure 4.7. In general the datapoints are non-separable since they overlap in the feature space.

There are some cluster characteristics which can be identified for each posture. The supine posture seems to have the lowest average kurtosis and is centered in skewness on both the feature plots. The kurtosis of the lateral 30° postures is closer towards the supine postures than to the lateral 90° postures, which tend to be highest in kurtosis. Opposing skewness is seen for the left and right lateral postures.

The location of mean of the simulated pressure distribution show an inverse linear relation for the skewness. Expressed in terms of an equation for a linear line $y = ax + b$ were skewness is y and the mean of the simulated pressure curve x, the postures data points seem to follow a similar negative factor for a and different offset values for b, were the b value for -90° postures is lowest, for 90° postures highest and centered for supine postures, with 30°postures in between.

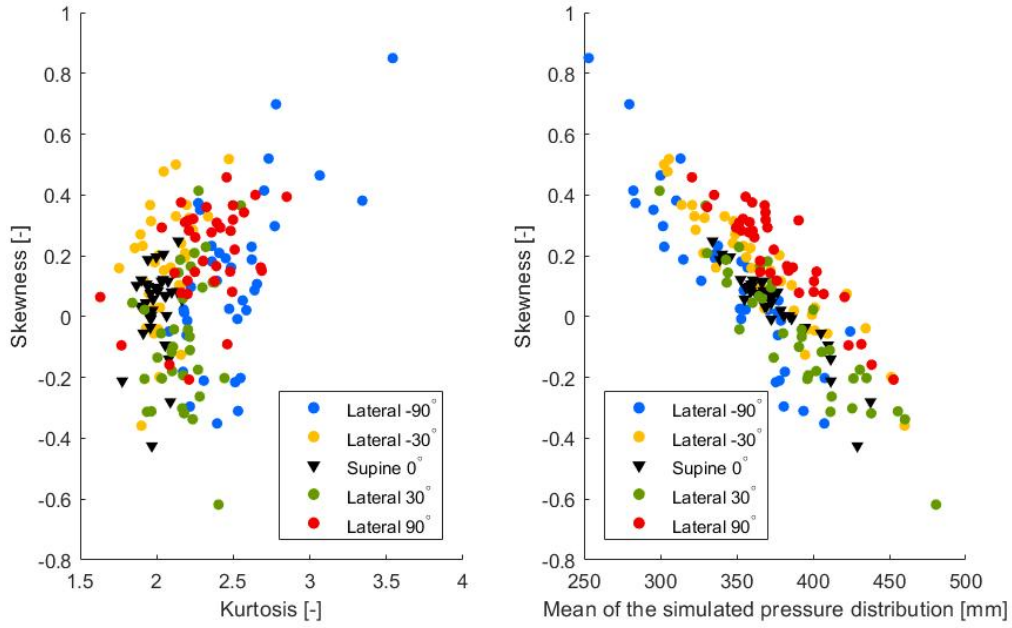

Figure 4.7: Feature scatter plots depicting skewness, kurtosis and the mean of the simulated pressure distribution, for subjects in the training dataset.

The data from the trainingset was used to train k-NN and SVM classification algorithms with the machine learning toolbox from Matlab, and compared to each other using 10-fold cross validation to select the best performing algorithms. The optimal classification algorithms were chosen from this dataset, one classifying three postures and one classifying five postures. The three posture classification algorithm could be useful for healthcare institutions that do not use the 30° posture in there repositioning protocol.

Based on the cross-validation accuracy, the SVM algorithms outperformed the k-NN algorithms. The maximal accuracy from cross validation was 69.5% and 94.4% for the three posture and five posture classifiers, were three posture classifier used a cubic Kernel function and the five posture classifier a linear Kernel. The accuracy difference was in general small for different Kernel functions.

Table 4.3: Confusion matrix in percentage for the five posture classifier.

		Predicted				
	Posture Class	-90°	-30°	0°	30°	90°
Actual	-90°	73.6	0	0	14.2	12.3
	-30°	0	63.4	0	14.6	22.0
	0°	0	16.4	75.2	3.6	4.9
	30°	1.2	10.4	26.4	61.9	0
	90°	0	0	0	8.3	91.6
	Recall	73.6	63.4	75.2	61.9	91.6
	Precision	98.1	70.7	72.9	60.8	70.5
	Accuracy			**73.1**		

The accuracy was determined by running the final classification algorithms on the test set. Since it is desired to determine the classification accuracy in time, the classifier is tested on the entire dataset for the four subjects when the subject is not moving and the posture is known. This gives an indication on the robustness of the classifier. The result is displayed in two confusion matrices, given for five postures in table 4.2 and for three postures in 4.2. The confusion matrix gives insight in what postures are predicted correct and which were misclassified, where the true postures are the first column and the predicted postures the first row. Accuracy is the percentage of postures correctly classified divided over the total amount of predictions, given by the formula $(TP + TN)/(TP + FP + FN + TN)$. The recall for a class is the percentage of times that a posture was correctly predicted out of the total actual posture cases for that class, calculated by $TP/(TP + FN)$. Precision is the percentage of postures that is correctly predicted out the total instances that posture is predicted, calculated by $TP/(TP + FP)$. Where TP, FP and FN stand for true positive, false positive and false negative.

Table 4.4: Confusion matrix in percentage for the three posture classifier.

		Predicted		
	Posture Class	-90°	0°	90°
Actual	-90°	86.5	1.3	12.3
	0°	0.2	75.3	24.5
	90°	9.3	0	90.7
	Recall	86.5	75.3	90.7
	Precision	89.9	98.3	72.1
	Accuracy		**84.3**	

Chapter 5

Discussion

The main goal of this thesis was to design a sensor system meeting clinical requirements for pressure ulcer prevention and determine the posture classification accuracy. This pilot study trained an algorithm on pressure data from 18 subjects and tested on data from 4 other subjects, which resulted in a classification accuracy of 84.3% for three postures. This suggests that posture classification for different persons is possible by measuring their pressure profile underneath a mattress, yet with a small error range.

5.1 Attained Requirements

The clinical requirements of cost effectiveness, patient non-intrusiveness, hospital bed compatibility and compatibility with all patient types, were leading in the design of the sensor system. Firstly, cost effectiveness was reached by developing a standalone device using a limited amount of only 24 force sensing resistors to reduce the hardware costs. Secondly, patient non-intrusiveness is achieved by the sensor system being a thin piece of plate material of only 11mm thick. Although this was not directly tested in the experiments with the sensor system, a small test with one test subject was conducted using a similar sized plate material of 10mm thick, which the test subject did not feel underneath the mattress. Thirdly it is assumed to be compatible with the majority of hospital beds since hospital beds have a rigid and flat bedframe, however further testing is necessary to validate this assumption. Fourthly the force range of the FSR's are selected based on a patient weight range requirement of 30kg and 170kg, however the model classification accuracy cannot be extrapolated to patients of this weight range, since the weight range of the test subjects included is limited and unevenly distributed.

The clinical requirements for compatibility with current pressure ulcer prevention strategies were analysed during the experiments. The compatibility with varying mattress types was investigated during the first experiment, were the feature space of two subjects measured on a foam mattress was compared with the feature space of the same subjects on an air mattress. The feature spaces showed cluster characteristics according to the hypothesis for each mattress individually, however they did not overlap. This was probably caused by mattress differences in stiffness and pressure propagating properties, as the air mattress was noticeably stiffer than the foam mattress. These two effects likely caused the higher kurtosis for all postures on the air mattress resulting in the air mattress feature space being a scaled version of the foam mattress feature space. Due to this

scaling factor per mattress type, it is preferred to train a classification algorithm on one mattress type to increase performance.

The last requirement was to be able to distinguish five postures relevant for the repositioning practice, which included the 30° lateral postures. A reasonably good classification accuracy for five postures of 73.1% was achieved. As expected the performance is lower than three posture classification, due to the increased classification difficulty of adding two added classes in an overlapping feature space. Recall was lowest for the two 30° lateral postures, meaning that these postures had the highest misclassification rate.

5.2 Classification Model Evaluation

Apart from accuracy, the classification model performances are further indicated by the recall and the precision given for each predicted posture class. Since a patient is expected to be repositioned an equal amount of times on every posture, correct classification of each posture is equally important. This means that recall is preferred to be similar between classes. Furthermore it is preferred that the precision is similar to the recall for that class, otherwise this is an indication that there is a bias in the classification algorithm.

Examining the confusion matrix for the three posture classifier, some spread in the recall for the posture classes is seen. The supine 0° posture has the lowest recall, meaning has the most difficulty detecting that class. However it has the highest precision, meaning that when a supine posture is detected, the model is almost always right. The opposite holds for the right lateral 90° posture, which has a high recall yet low precision. This indicates that the right lateral 90° posture is detected most often and the classification model is biased towards that class, meaning that the classification algorithm is not entirely balanced and can be further improved.

5.3 Comparison to other Posture Classification Methods

It is interesting to compare the classification results of this thesis to three other methods identified in the background research: the low resolution sensor array on top of the mattress, the high resolution sensor mats on top of the mattress and the accelerometer taped to the chest of the patient.

The affordable low resolution sensor mat on top of the mattress that was developed by Hsia et al. (2008) reached an accuracy of 78% [24]. They used a different experiment methodology, so the results cannot be precisely compared, yet the results of this thesis match in order of magnitude, meaning that measuring underneath the mattress is a valid alternative for measuring on top of the mattress for posture classification. Posture classification accuracy for high resolution sensor mats can be seen in table 2.2 and are generally around 97%. Such a system is quite expensive and the sensor mat is generally less comfortable than a regular mattress. Pickham et al. (2017) used the accelerometer taped on a chest to classify posture in their randomised controlled trial [43]. No accuracy is given, but an angle threshold was used. Since this angle is in direct relation to the posture, it is assumed that this reaches a very high classification accuracy. An accelerometer is furthermore relatively affordable, however this system cannot be reused for new patients and it is intrusive to the patient.

An erroneous posture classification increases the risk for pressure ulcers, however it does not directly mean that a pressure ulcer will develop, as there are many patient individual factors that play a role. For the patient group with the highest pressure ulcer risk, it is probably more beneficial

to use a more accurate method for posture classification, like the accelerometer or the high resolution sensor mat. Because their threshold for mechanical load in time is lower, it is more important that the classification is correct. For patients that are slightly less at risk, the system that is developed in this thesis might be more beneficial due to the cost effectiveness and non-intrusiveness for the patient.

5.4 Strengths and Limitations

The focus of this thesis was on the patient, caregiver and the compatibility with current pressure ulcer prevention strategies. One of the strengths was the broad research scope, starting from a medical background going intro electrical, mechanical and algorithm development. This broad scope was important to identify the main requirements for the sensor development.

Current literature on posture classification using force sensing resistors, used the sensors to measure pressure on top of the mattress. This research is one of the first that attempted posture classification with force sensing resistors placed underneath a mattress. The design methodology is structurally described and ways to improve the sensor signal are proposed, such as the incorporation the center of pressure on the pressure capturing plates, to improve the representation of the force curve and embedding the sensors into a frame to increase the measured surface area and to constrain unwanted loading conditions. The experiments were designed to analyse several situations in clinical practice, were there are different bed types, patients types and the lateral 30° posture is used. Test subjects were only told to lie in a specific angle, they were free to interpret this to their usual lying posture in order to be close to a real situation.

It is however also important to state the limitations of this research. First of all the testing time did not represent a real situation, since test subjects were a maximum of one minute in one posture and were in a test environment, which could have influenced their posture. The data set gathered is small and conducted on healthy test subject, so the demographics of the included subjects do not reflect those of patients at risk of pressure ulcer development. This suggest that the classification model is likely overfitted to the training set. Only two standard classification algorithms were used due to the limited data available and more data would give options for advanced classification algorithms.

During the material selection of the sensor plate there was high emphasis on manufacturability of plate material around the thickness range of 5mm at high tolerance and therefore the material PMMA was chosen. PMMA works in terms of stiffness, however with advanced production methods it is also possible with aluminium or steel, so a larger measuring area or thinner system can be obtained.

The optimal measuring location of the sensor system was reasoned to be underneath the chest, but this was not further investigated during this research. A downside from the fact that subjects could choose their posture, is that it is unclear what the effects of arm placements and alignment of the body with the mattress are.

Little was known about the pressure distribution underneath the mattress. The sensor was designed to detect the hypothesized signals present in the pressure distribution underneath the mattress at the location of the upper chest. The sensor design parameters were based on measurements with a relatively low accurate sensor. Using a pressure matt underneath the whole surface area of the mattress might be a suitable way of researching more optimal locations of a similar sensor system.

5.5 Recommendations

For future research using this sensor system, it is interesting to investigate the classification performance over a broader test subject weight range, more mattress types, a longer period in time and other sensor plate locations. Furthermore literature indicates that measuring vibration from heartbeat and respiration could be useful for posture detection [4, 39]. Combining piezoceramic sensors with force sensing resistors might be a way to measure both pressure distribution as well as vibrations, so combining those features in a posture classification algorithm could increase the classification accuracy.

The sensor and algorithm combination described in this thesis were based on static pressure distributions. For pressure ulcer prevention it is necessary to expand this algorithm so that it can track the posture in time. This could also allow for some accuracy increase, if for example a standard repositioning posture protocol can be incorporated in the machine learning process.

Other than a general pre-trained classification algorithm, it is interesting to investigate possibilities for a personalized learning approach, since the best accuracy will be obtained if an algorithm matches a specific patient and mattress combination. For example, this could be achieved by having an initial learning protocol when deploying a system with a new patient, or if the system would receive posture information from the caregiver each time a reposition is performed.

Chapter 6

Conclusions

In conclusion, a sensor design meeting most clinical requirements for pressure ulcer prevention was developed and the pilot study showed a good bed posture classification result from an experiment with one foam mattress. This suggest the feasibility for posture classification using a limited amount of force sensing resistors placed underneath the mattress.

The results indicated that the force signal and its features are different for a foam and an air mattress, meaning that the best classification accuracy will be obtained if the classification model is designed and used with one specific mattress type. More research is needed on how the accuracy can be further improved and how a classification model would perform on a large data set covering very light and heavy test subjects.

For pressure ulcer prevention, there are alternative methods that obtain a higher posture classification accuracy. For the patient group with the highest pressure ulcer risk, it is probably more beneficial to use a more accurate method, because their threshold for mechanical load in time is lower, so it is more important that the classification is correct. For patients that are slightly less at risk, the system that is developed in this thesis might be a useful alternative due to the cost effectiveness and non-intrusiveness for the patient.

Appendix A

Data of Experiment Two

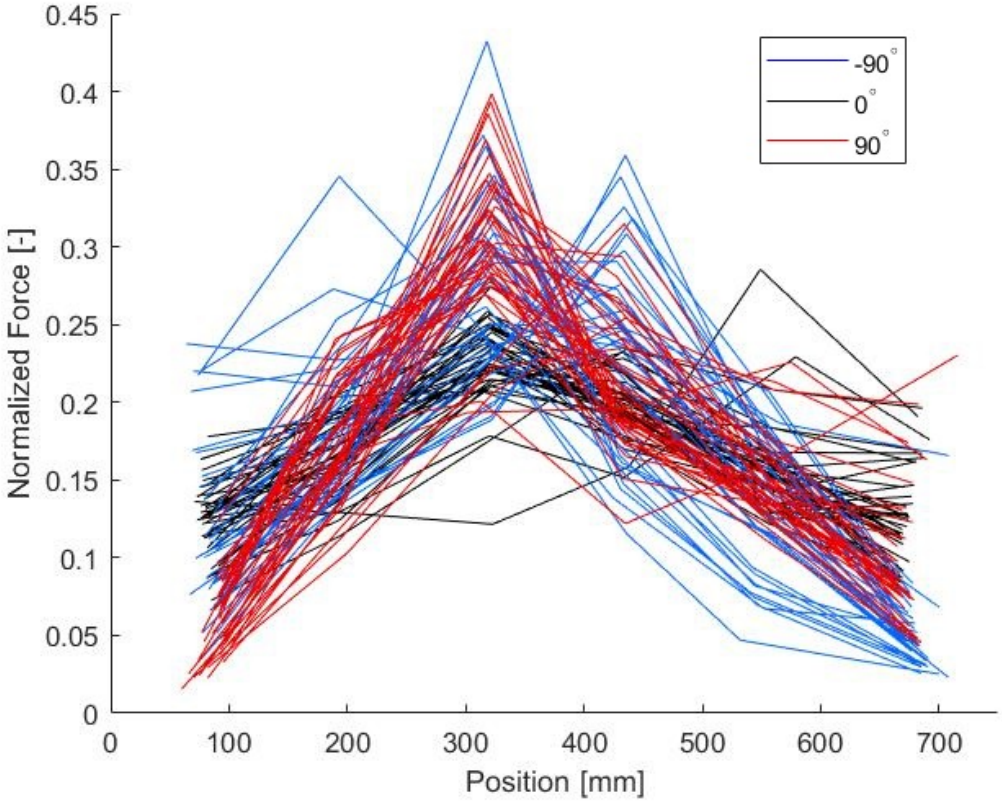

Figure A.1: All force graphs for supine and lateral 90° postures in the training set.

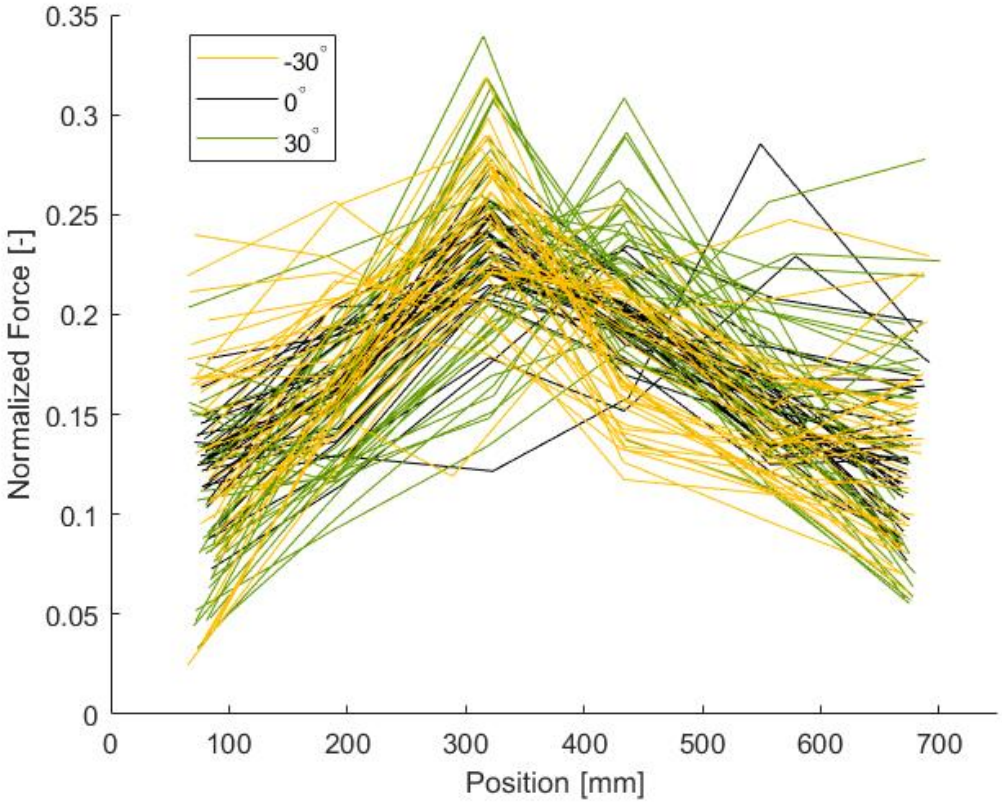

Figure A.2: All force graphs for supine and lateral 30° postures in the training set.

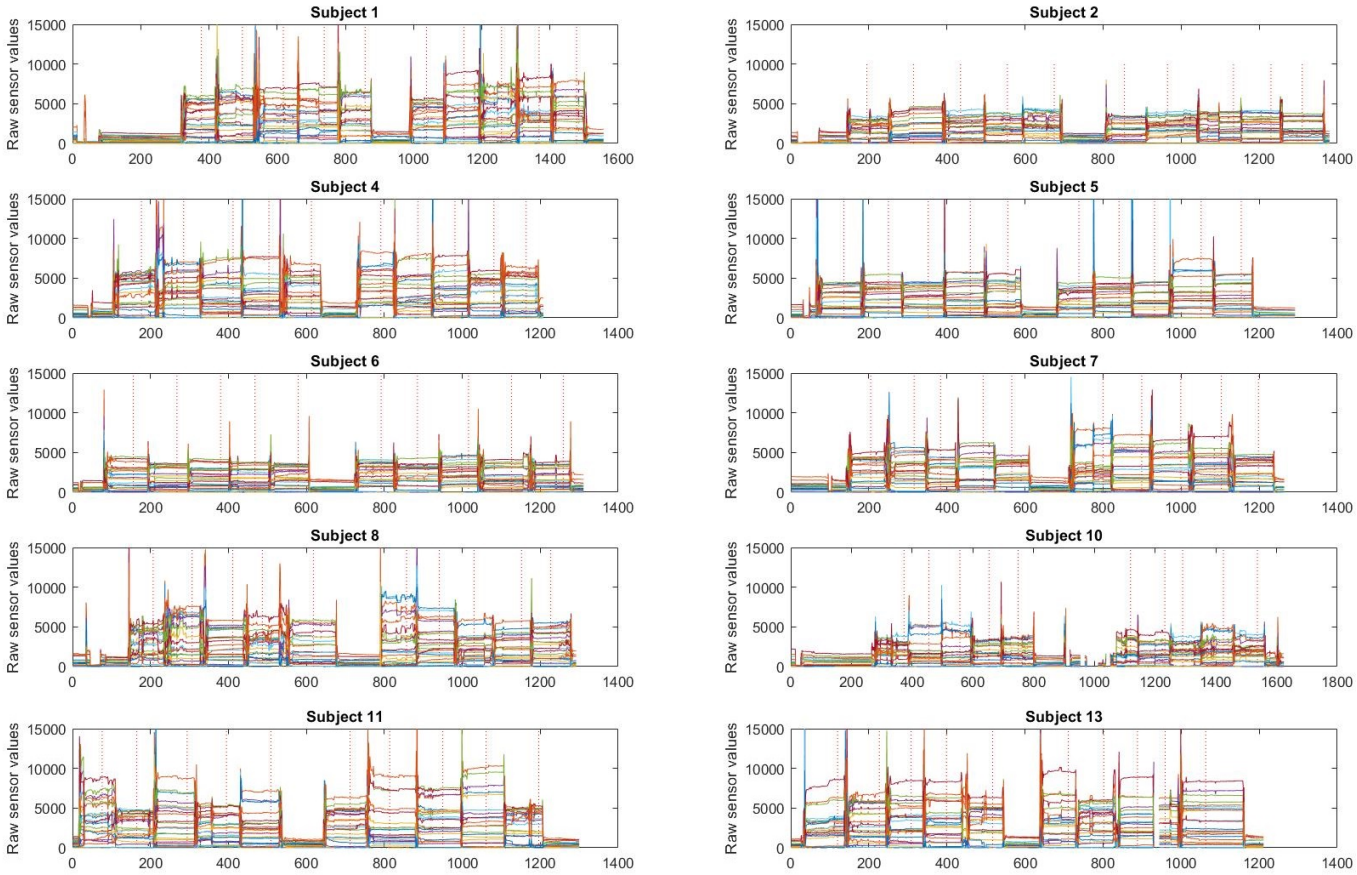

Figure A.3: Raw sensor readings for the first 10 subjects in the training set. The vertical line indicates the sample that is taken as a label for that posture, where the sample number is given on the x axis.

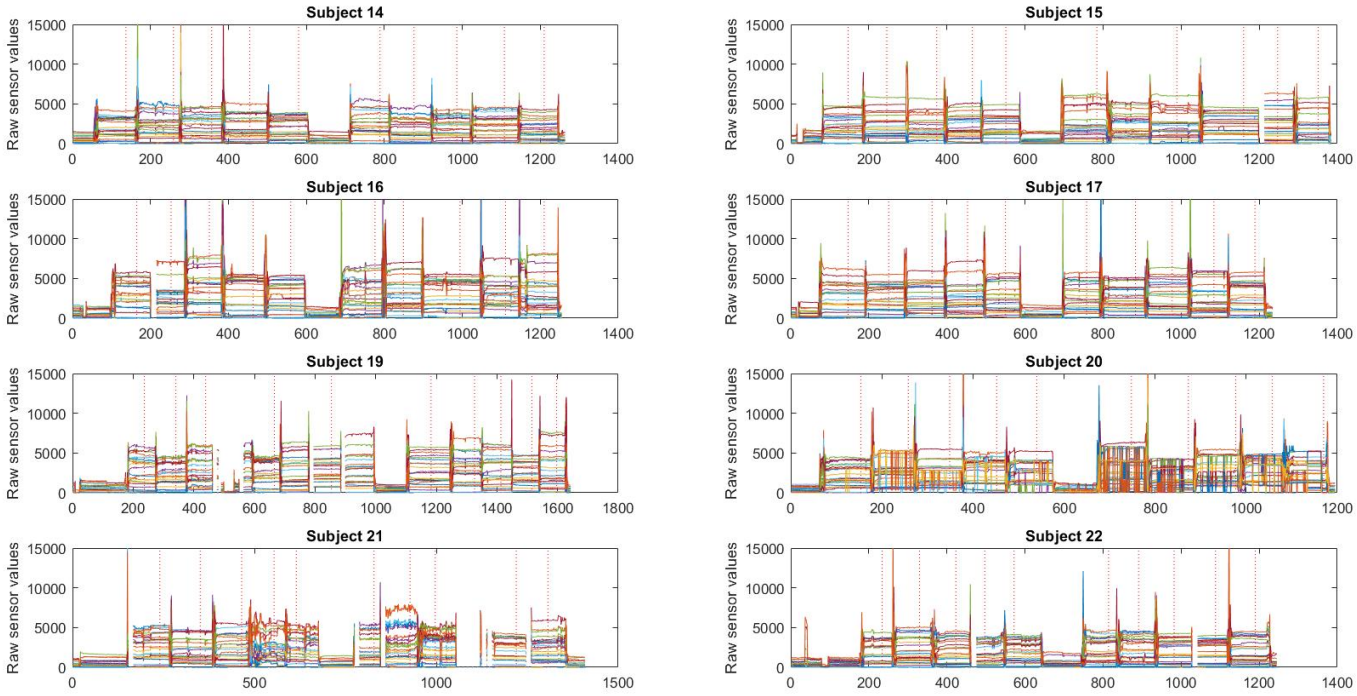

Figure A.4: Raw sensor readings for the last 8 subjects in the training set. The vertical line indicates the sample that is taken as a label for that posture, where the sample number is given on the x axis.

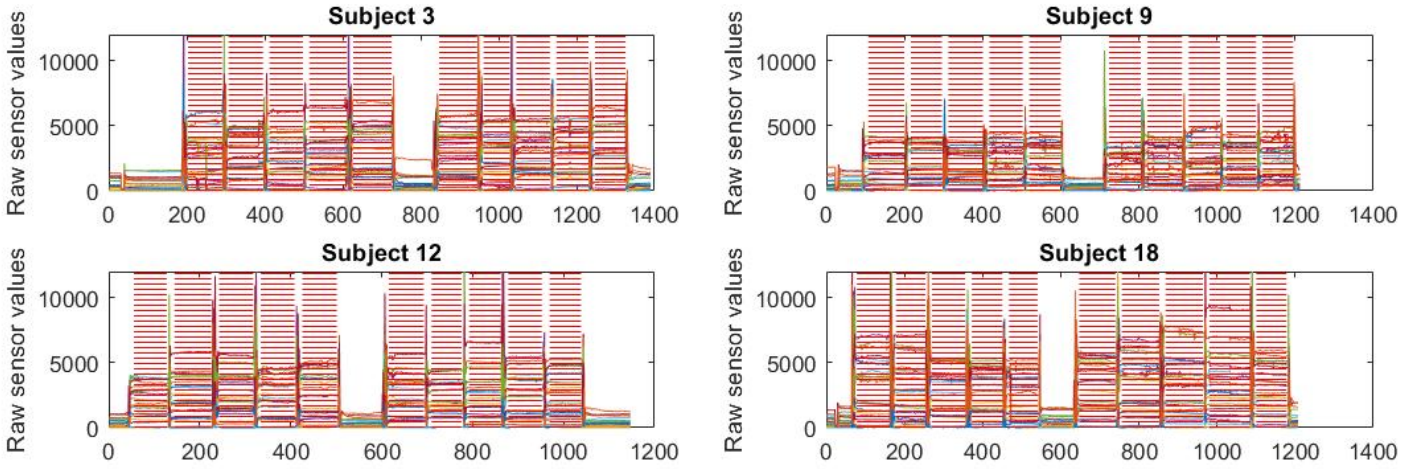

Figure A.5: Raw sensor readings for the 4 subjects in the test set. The classification algorithm was used to classify the posture during the whole period the subject was laying still. This is indicated by the vertical lines, where the sample number is given on the x axis.

Bibliography

[1] http://www.precision-crop-protection.uni-bonn.de/gk_research/project_3_06/image_3.jpg.

[2] *National Pressure Ulcer Advisory Panel, European Pressure Ulcer Advisory Panel and Pan Pacific Pressure Injury Alliance. Prevention and treatment of pressure ulcers: clinical practice guideline.* Emily Haesler (Ed.), Cambridge Media: Osborne Park, Western Australia, 2014.

[3] a. Adami, T. Hayes, M. Pavel, and C. Singer. Detection and Classification of Movements in Bed using Load Cells. *Annual International Conference of the IEEE Engineering in Medicine and Biology Society. IEEE Engineering in Medicine and Biology Society. Conference*, 1:589–92, 2005.

[4] Z. T. Beattie, C. C. Hagen, and T. L. Hayes. Classification of lying position using load cells under the bed. *Proceedings of the Annual International Conference of the IEEE Engineering in Medicine and Biology Society, EMBS*, pages 474–477, 2011.

[5] B. R. Behrendt, A. M. Ghaznavi, M. Mahan, S. Craft, and A. Siddiqui. Continuous Bedside Pressure Mapping and Rates of Hospital-Associated Pressure Ulcers in a Medical Intensive Care Unit. 23(2):127–133, 2014.

[6] N. Bergstrom, B. Braden, M. Kemp, M. Champagne, E. Ruby, D. R. Berlowitz, G. H. Brandeis, J. Anderson, W. Du, H. Brand, J. Black, M. M. Baharestani, J. Cuddigan, B. Dorner, L. Edsberg, D. Langemo, M. E. Posthauer, C. Ratliff, G. Taler, Others, G. H. Brandeis, J. N. Morris, D. J. Nash, L. A. Lipsitz, B. Dorner, M. E. Posthauer, D. R. Thomas, Others, A. Gefen, N. Graves, F. Birrell, M. Whitby, P. Guenter, R. Malyszek, D. Z. Bliss, T. Steffe, Others, J. M. Guralnik, T. B. Harris, L. R. White, J. C. Cornoni-Huntley, S. D. Horn, S. A. Bender, M. L. Ferguson, R. J. Smout, N. Bergstrom, G. Taler, A. S. Cook, S. S. Sharkey, A. C. Voss, M. Kosiak, F. G. Marchione, L. M. Q. V. M. Q. V. Araújo, L. M. Q. V. M. Q. V. Araújo, E. M. H. Mathus-Vliegen, E. McInnes, A. Jammali-Blasi, S. Bell-Syer, J. Dumville, N. Cullum, E. P. U. A. P. National Pressure Ulcer Advisory Panel, P. P. P. I. Alliance, W. V. Padula, M. K. Mishra, M. B. F. Makic, P. W. Sullivan, M. Reddy, S. S. Gill, P. a. Rochon, J. B. Reuler, T. G. Cooney, J. L. Severens, J. M. Habraken, S. Duivenvoorden, C. M. A. Frederiks, and D. R. Thomas. Multi-site study of incidence of pressure ulcers and the relationship between risk level, demographic characteristics, diagnoses, and prescription of preventive interventions. *Advances in skin & wound care*, 52(5):661–666, 2006.

[7] N. Bergstrom, S. D. Horn, M. P. Rapp, A. Stern, R. Barrett, and M. Watkiss. Turning for ulcer ReductioN: A Multisite randomized clinical trial in nursing homes. *Journal of the American Geriatrics Society*, 61(10):1705–1713, 2013.

[8] D. R. Berlowitz, G. H. Brandeis, J. Anderson, W. Du, and H. Brand. Effect of pressure ulcers on the survival of long-term care residents. *The Journals of Gerontology Series A: Biological Sciences and Medical Sciences*, 52(2):M106—-M110, 1997.

[9] J. M. Black, L. Edsberg, M. Baharestani, D. Langemo, M. Goldberg, L. McNichol, J. Cuddigan, and t. N. P. U. A. Panel. Pressure ulcers: avoidable or unavoidable? Results of the National Pressure Ulcer Panel consensus conference. *Ostomy Wound Management*, 57(2):24–37, 2011.

[10] S. Coleman, C. Gorecki, E. A. Nelson, S. J. Closs, T. Defloor, R. Halfens, A. Farrin, J. Brown, L. Schoonhoven, and J. Nixon. Patient risk factors for pressure ulcer development: Systematic review. *International Journal of Nursing Studies*, 50(7):974–1003, 2013.

[11] S. Coleman, J. Nixon, J. Keen, L. Wilson, E. Mcginnis, C. Dealey, N. Stubbs, A. Farrin, D. Dowding, J. M. Schols, J. Cuddigan, D. Berlowitz, E. Jude, P. Vowden, L. Schoonhoven, D. L. Bader, A. Gefen, C. W. Oomens, and E. A. Nelson. A new pressure ulcer conceptual framework. *Journal of Advanced Nursing*, 70(10):2222–2234, 2014.

[12] K. F. de Oliveira, K. G. Nascimento, A. C. Nicolussi, S. R. R. Chavaglia, C. A. de Araújo, and M. H. Barbosa. Support surfaces in the prevention of pressure ulcers in surgical patients: An integrative review. *International Journal of Nursing Practice*, 23(4):e12553, 2017.

[13] B. de Wilde. http://bdewilde.github.io/blog/blogger/2012/10/26/classification-of-hand-written-digits-3/. 2012.

[14] B. Dorner, M. E. Posthauer, D. Thomas, and Others. The role of nutrition in pressure ulcer prevention and treatment: National Pressure Ulcer Advisory Panel white paper. *Advances in skin & wound care*, 22(5):212–221, 2009.

[15] Epsilonengineer. https://www.epsilonengineer.com/uploads/7/1/6/9/71698693/_1342692_orig.png.

[16] N. Foubert, A. M. McKee, R. A. Goubran, and F. Knoefel. Lying and sitting posture recognition and transition detection using a pressure sensor array. *Medical Measurements and Applications Proceedings (MeMeA), 2012 IEEE International Symposium on*, pages 1–6, 2012.

[17] A. Gefen, B. van Nierop, D. L. Bader, and C. W. Oomens. Strain-time cell-death threshold for skeletal muscle in a tissue-engineered model system for deep tissue injury. *Journal of Biomechanics*, 41(9):2003–2012, 2008.

[18] B. M. Gillespie, W. P. Chaboyer, E. McInnes, B. Kent, J. A. Whitty, and L. Thalib. Repositioning for pressure ulcer prevention in adults (Review). *Cochrane Database of Systematic Reviews*, (4):1–42, 2014.

[19] N. Graves, F. Birrell, and M. Whitby. Effect of pressure ulcers on length of hospital stay. *Infection Control & Hospital Epidemiology*, 26(3):293–297, 2005.

[20] L. Gunningberg, I. M. Sedin, S. Andersson, and R. Pingel. Pressure mapping to prevent pressure ulcers in a hospital setting: A pragmatic randomised controlled trial. *International Journal of Nursing Studies*, 72(March):53–59, 2017.

[21] T. Harada and T. Mori. Estimation of Bed-Ridden Human's Gross and Slight Movement Based on Pressure Sensors Distribution Bed Tatsuya. (May):3795–3800, 2002.

[22] M. Heydarzadeh, M. Nourani, and S. Ostadabbas. In-bed posture classification using deep autoencoders. *Proceedings of the Annual International Conference of the IEEE Engineering in Medicine and Biology Society, EMBS*, 2016-Octob:3839–3842, 2016.

[23] S. D. Horn, S. A. Bender, M. L. Ferguson, R. J. Smout, N. Bergstrom, G. Taler, A. S. Cook, S. S. Sharkey, and A. C. Voss. The national pressure ulcer long-term care study: pressure ulcer development in long-term care residents. *Journal of the American Geriatrics Society*, 52(3):359–367, 2004.

[24] C. C. Hsia, Y. W. Hung, Y. H. Chiu, and C. H. Kang. Bayesian classification for bed posture detection based on kurtosis and skewness estimation. *2008 10th IEEE Intl. Conf. on e-Health Networking, Applications and Service, HEALTHCOM 2008*, pages 165–168, 2008.

[25] C. C. Hsia, K. J. Liou, A. P. W. Aung, V. Foo, W. Huang, and J. Biswas. Analysis and Comparison of Sleeping Posture Classification Methods using Pressure Sensitive Bed System. *2009 Annual International Conference of the Ieee Engineering in Medicine and Biology Society, Vols 1-20*, pages 6131–6134, 2009.

[26] M. Kagawa, K. Ueki, H. Tojima, and T. Matsui. Noncontact screening system with two microwave radars for the diagnosis of sleep apnea-hypopnea syndrome. *Conference proceedings : ... Annual International Conference of the IEEE Engineering in Medicine and Biology Society. IEEE Engineering in Medicine and Biology Society. Annual Conference*, 2013:2052–2055, 2013.

[27] M. Kosiak. Etiology of decubitus ulcers. *Archives of physical medicine and rehabilitation*, 42:19–29, 1961.

[28] E. Linder-Ganz, N. Shabshin, Y. Itzchak, and A. Gefen. Assessment of mechanical conditions in sub-dermal tissues during sitting: A combined experimental-MRI and finite element approach. *Journal of Biomechanics*, 40(7):1443–1454, 2007.

[29] J. J. Liu, W. Xu, M. C. Huang, N. Alshurafa, M. Sarrafzadeh, N. Raut, and B. Yadegar. A dense pressure sensitive bedsheet design for unobtrusive sleep posture monitoring. *2013 IEEE International Conference on Pervasive Computing and Communications, PerCom 2013*, (March):207–215, 2013.

[30] C. H. Lyder. Pressure Ulcer Prevention and Management. *Jama*, 289(2):223, 2003.

[31] Mangarhealth. https://mangarhealth.com/news/the-prevention-of-pressure-ulcers/. 2018.

[32] F. G. Marchione, L. M. Q. Araújo, and L. V. Araújo. Approaches that use software to support the prevention of pressure ulcer: A systematic review. *International Journal of Medical Informatics*, 84(10):725–736, 2015.

[33] E. M. H. Mathus-Vliegen. Clinical observations: nutritional status, nutrition, and pressure ulcers. *Nutrition in Clinical Practice*, 16(5):286–291, 2001.

[34] E. Mcinnes, B.-s. Sem, D. Jc, V. Middleton, and N. Cullum. Support surfaces for pressure ulcer prevention (Review). (9), 2015.

[35] E. H. Moore Zena and S. Cowman. Risk assessment tools for the prevention of pressure ulcers. *Cochrane Database of Systematic Reviews*, (2), 2014.

[36] S. Motamedi, J. de Grood, S. Harman, P. Sargious, B. Baylis, W. Flemons, and W. Ghali. The effect of continuous pressure monitoring on strategic shifting of medical inpatients at risk for PUs. *Journal of Wound Care*, 21(11):517–527, nov 2012.

[37] K. Nakajima, Y. Matsumoto, and T. Tamura. Development of real-time image sequence analysis for evaluating posture change and respiratory rate of a subject in bed. *Physiological Measurement*, 22(3):20–28, 2001.

[38] D. Nayak, K. Srinivasan, S. Jagdish, R. Rattan, and V. S. Chatram. Bedsores: "Top to bottom" and "bottom to top". *Indian Journal of Surgery*, 70(4):161–168, 2008.

[39] S. Nukaya, T. Shino, Y. Kurihara, K. Watanabe, and H. Tanaka. Noninvasive bed sensing of human biosignals via piezoceramic devices sandwiched between the floor and bed. *IEEE Sensors Journal*, 12(3):431–438, 2012.

[40] C. W. J. Oomens, D. L. Bader, S. Loerakker, and F. Baaijens. Pressure Induced Deep Tissue Injury Explained. *Annals of Biomedical Engineering*, 43(2):297–305, 2015.

[41] OpenMusicLabs. FSR tutorial.

[42] S. Ostadabbas, M. Baran Pouyan, M. Nourani, and N. Kehtarnavaz. In-bed posture classification and limb identification. *IEEE 2014 Biomedical Circuits and Systems Conference, BioCAS 2014 - Proceedings*, pages 133–136, 2014.

[43] D. Pickham, N. Berte, M. Pihulic, A. Valdez, B. Mayer, and M. Desai. Effect of a Wearable Patient Sensor on Care Delivery for Preventing Pressure Injuries in Acutely Ill Adults: A Pragmatic Randomized Clinical Trial (LS-HAPI Study). *International Journal of Nursing Studies*, 80(June 2017):12–19, 2017.

[44] M. B. Pouyan, S. Ostadabbas, M. Farshbaf, R. Yousefi, and M. Nourani. Continuous Eight-Posture Classification for Bed-Bound Patients. (Bmei):121–126, 2013.

[45] M. Reddy, S. S. Gill, and P. a. Rochon. Preventing pressure ulcers: a systematic review. *Jama*, 296(8):974–984, 2006.

[46] B. S. Renganathan, S. P. Preejith, S. Nagaiyan, J. Joseph, and M. Sivaprakasam. A novel system to tackle hospital acquired pressure ulcers. *Proceedings of the Annual International Conference of the IEEE Engineering in Medicine and Biology Society, EMBS*, 2016-Octob:4780–4783, 2016.

[47] J. B. Reswick and J. E. Rogers. Experience at Rancho Los Amigos Hospital With Devices and Techniques to Prevent Pressure Sores. In *Bed Sore Biomechanics*, pages 301–310. Macmillan Education UK, London, 1976.

[48] J. B. Reuler and T. G. Cooney. The pressure sore: pathophysiology and principles of management. *Annals of Internal Medicine*, 94(5):661–666, 1981.

[49] J. L. Severens, J. M. Habraken, S. Duivenvoorden, and C. M. A. Frederiks. The cost of illness of pressure ulcers in The Netherlands. *Advances in skin & wound care*, 15(2):72–77, 2002.

[50] A. Siddiqui, R. Behrendt, M. Lafluer, and S. Craft. A Continuous Bedside Pressure Mapping System for Prevention of Pressure Ulcer Development in the Medical ICU: A Retrospective Analysis. 25(12):234–241, 2013.

[51] Tekscan. https://www.tekscan.com/sites/default/files/flexiforce-a301-force-sensor_0.jpg.

[52] Tekscan. Flexiforce a301 Datasheet: https://www.tekscan.com/resources/product/flexiforce-a301-datasheet. Technical report, 2018.

[53] Tekscan. The Difference Between Force Measurement Techniques. Technical report, 2018.

[54] J. P. Tran, J. M. McLaughlin, R. T. Li, and L. G. Phillips. Prevention of Pressure Ulcers in the Acute Care Setting: New Innovations and Technologies. *Plastic and Reconstructive Surgery*, 138:232S–240S, 2016.

[55] G. S. Walia, A. L. Wong, A. Y. Lo, G. A. Mackert, H. M. Carl, R. A. Pedreira, R. Bello, and C. S. Aquino. Efficacy of Monitoring Devices in Support of Prevention of Pressure Injuries: Systematic Review and Meta-analysis. *Advances in skin & wound care*, 29(December):1364–1371, 2016.

[56] R. Yousefi, S. Ostadabbas, M. Faezipour, M. Farshbaf, M. Nourani, L. Tamil, and M. Pompeo. Bed posture classification for pressure ulcer prevention. *Proceedings of the Annual International Conference of the IEEE Engineering in Medicine and Biology Society, EMBS*, pages 7175–7178, 2011.

[57] M. Zeh, Z. E. Moore, and S. Cowman. Repositioning for treating pressure ulcers (Review) Repositioning for treating pressure ulcers. *The Cochrane database of systematic reviews*, (1), 2015.

[58] J. L. Zeller, C. Lynm, and R. M. Glass. Pressure Ulcers. *JAMA*, 296(8):1020, aug 2006.